THE FUNDAMENTAL FLAWS OF THE WAXMAN-SMITS AND DUAL WATER FORMULATIONS, ATTEMPTED REMEDIES, AND NEW REVELATIONS FROM HISTORICAL LABORATORY COMPLEX CONDUCTIVITY MEASUREMENTS

John Rasmus, David Kennedy, Dean Homan

This paper was prepared for presentation at the SPWLA 64th Annual Logging Symposium held in Lake Conroe, TX, USA, June 10-14, 2023.

ABSTRACT

The Waxman-Smits formula was introduced in 1968 as a parallel conductance model to improve previous models. A careful inspection of Waxman's and Smits model reveals it is not a parallel conduction model by the conventional definition.

First, Waxman-Smits assumed that "the electrical current transported by the counterions associated with the clay travels along the same tortuous path as the current attributed to the ions in the pore water" , (Waxman-Smits 1968) removing an essential feature of a parallel conduction model, that there be two separate conductors. Based on this assumption they assign the same geometrical factor to both current paths. The geometrical factor is defined as the reciprocal of the formation resistivity factor ($1/F$ or φ^m). Waxman-Smits found experimentally that a shaly sand appeared to have an F that was larger than a clean sand and introduced F^* to account for this. Therefore, the tortuosity of the current paths through the clay and the pore water were deemed to be equivalent, with both tortuosity's increasing equally as the clay content increased.

Second, a parallel model requires the bulk conductivity of a volume be weighted by the fractional volumes of the separate clay and interstitial water current paths. Clavier et al. (1977) discovered during the field testing of the new 1.1 GHz electromagnetic propagation tool that there existed a volume of clay water of near constant salinity in shales. These two concepts are not accounted for in the Waxman-Smits model. A re-evaluation of the Waxman-Smits database by Clavier et al. revealed the F^* increase was primarily due to the Waxman-Smits model not accounting for the physical presence of the volume of the clay water. The inclusion of the clay water volume in the Dual Water Model produces a true parallel conductivity model. However, like Waxman-Smits, it assigns the same tortuosity to both the clay and pore water current paths.

This assumption seems dubious based on observations of Scanning Electron Microscope (SEM) photos showing actual clay morphologies. Laboratory measurements of pure clay and glass beads would allow one to quantify tortuosity changes due to the introduction of clay into an otherwise pure glass bead environment.

Theoretically and experimentally, the value of the clay water conductivity (C_{cw}) at room temperature was found to be 6.8 S/m. Therefore, for a pore-water conductivity (C_w) less than 6.8, the clay adds to the rock conductivity relative to an Archie rock as written in the Waxman-Smits model. However, when C_w is greater than 6.8, the clay water subtracts from the rock conductivity relative to an Archie rock. This cannot be accommodated by the Waxman-Smits formulation. To correct for this model deficiency, B was made a function of salinity and temperature when theoretically it is a function of temperature only.

Thirdly, neither model accurately predicts the rock conductivity at pore water salinities below approximately 0.5-1 S/m. Having a proper model at these lower salinities is important for geothermal evaluations, water flooded reservoirs and naturally occurring fresh-water reservoirs. We propose a correction method based on our knowledge gained from the study of the quadrature conductivity measurement from cores and recent laboratory measurements.

INTRODUCTION

The reader is encouraged to become familiar with Clavier et al., (1977, 1984) and Waxman-Smits (1968) shaly sand petrophysical models before reading this paper. An overview of the Waxman-Smits (WS) and Dual Water (DW) models follows. We concentrated on the analysis of the 27 core samples from group 2 shown in Table 7 of Waxman-Smits (1968) because WS considered them to be "the most accurate and complete with respect to range of Q_v and C_w values examined" (Waxman-Smits 1968) They also have the additional measurements of clay fraction types and percentages which we have determined are important. These values are given in the header of Table 2. We use the same nomenclature for the sample numbers as listed in Table 7 of Waxman-Smits (1968).

Review of WS Theory

Readers are familiar with the WS equation

$$C_t = \frac{S_{WT}^n}{F^*}\left[C_w + \frac{BQ_v}{S_{WT}}\right] \quad (1)$$

where C_t (S/m) is measured conductivity, S_{WT}^n (v/v) is total water saturation, F^* is the formation factor, C_w (S/m) is pore or non-clay water conductivity, B is clay molar counterion conductivity ((S/m)/(meq/cm^3)), and Q_v (meq/cm^3) is the concentration of clay counterions per unit pore volume. $Q_v = Q_{v\_chemical}$ is computed from the bulk cation exchange capacity (CEC) (meq/gm) measurements using

$$Q_{v\_chemical} = CEC\ \rho_g \left(\frac{1-\varphi_t}{\varphi_t}\right) \quad (2)$$

where ρ_g is the sample grain density and φ_t is total porosity.

Practical Implementation for Laboratory Measurements.

The core will be flooded with various values of pore water salinity having corresponding values of C_w, and conductivity measurements, C_0, taken at each salinity. For these laboratory measurements, Eq. (1) is simplified to

$$C_0 = \frac{1}{F^*}[C_w + BQ_v]. \quad (3)$$

Water conductivities of 20-25 S/m are a practical upper limit for C_w because the water at this value is close to being salt-saturated at room temperatures. 0.2 S/m is a useful lower limit for reasons shown later. F^* is then computed by taking the inverse slope of the C_0 vs. C_w data pairs using only the high salinity data. "High salinity" would correspond to a C_w greater than about 9-10 S/m and where we find the straight-line segment of the C_0 vs. C_w relationship. Waxman-Smits (1968) used up to 12 different C_w values ranging from 0.21 to 25 S/m in their experiments, Table 7, Waxman-Smits (1968). Q_v is measured by chemical methods independent of Eq. (3) and B was determined empirically by curve fitting the C_0 vs. C_w data to Eq. (3). B was initially given in equation form as a function of C_w (Eq. 19, Waxman-Smits 1968), then later modified to include the temperature effect (Waxman, 1974, 2007). Laboratory measurements at room temperature today typically use this updated correlation shown in Eq. 4 instead of deriving it experimentally.

$$B = 3.83 * [1 - 0.83\exp(-0.5C_w)] \quad (4)$$

The various components of the WS model in Eq. (1) are illustrated in Fig. 1 for Sample 26. The measured constants used in the WS model were $Q_v = Q_{v\_chem} = 1.47$, $\varphi = 0.229$, $m^* = 2.52$ ($F^* = 41$) and B as a function of C_w using Eq. (4). The model does not exactly fit the measured data. This is most likely the result of WS deriving the empirical constant B that best fit the group of samples they studied which means that it will not fit any of the individual samples exactly.

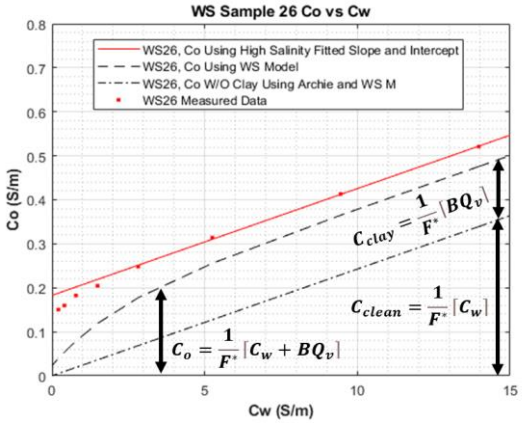

Fig. 1—WS model plotted with measured data illustrating the components of the WS model in Eq. 1.

Practical Implementation for Field Log Measurements.

Q_v cannot be measured directly and is therefore determined indirectly from gamma-ray, spontaneous potential, or other log measurements. Since F^* is also not available but porosity is, a correlation has been developed for cementation exponent, m^*, as a function of shaliness (illustrated in Fig. 3, Clavier et al. (1977)). By using the experimental data and

$$m^* = -\frac{Log\ F^*}{Log\ \varphi_t}, \quad (5)$$

a plot of m^* vs. Y or $\frac{Q_{v*}\varphi_t}{1-\varphi_t}$ yields

$$m^* = 1.75 + (1.128 * Y + 0.22 * (1 - e^{-17.3*Y}). \quad (6)$$

At this point, all the variables are known or measured for implementation into Eq. (1) for saturation calculations using log measurements.

Review of DW theory

The DW equation is given as

$$C_t = \frac{S_{WT}^n}{F_0}\left[C_w + \frac{v_Q Q_v (C_{cw} - C_w)}{S_{WT}}\right]. \quad (7)$$

where C_t (S/m) is measured conductivity, S_{WT}^n is total water saturation, F_0 is the formation factor, C_w (S/m) is pore or non-clay water conductivity, C_{cw} (S/m) is clay water conductivity, v_Q (cm^3/meq) is the clay water volume per meq, and Q_v (meq/cm^3) is the concentration of clay counterions per unit pore volume. Clay water refers to the water volume occupied by the adsorbed water on the clay surface and the hydrated compensating cations in the outer Helmholtz plane (OHP). As the pore water salinity decreases, these hydrated cations migrate out

into the pore space creating a diffuse layer having a volume that increases with decreasing pore water salinity.

The negative electrical charge associated with the clay that attracts the hydrated cations also repels some of the anions in the pore water.

The concentration of the clay water cations may be greater or less than the concentration of the cations in the pore water. This has important implications for the effective conductivity of clay water vs. pore water.

Clavier et al. (1977, 1984) introduce the concept of electrical Q_v or Q_{v_elect}. This is computed using Eq. (16), computed from the intercept, C_x, of the C_0-C_w crossplot using the linear, high salinity data. Q_{v_elect} provides a better fit to the measured data than the laboratory derived chemical Q_v or Q_{v_chem} computed from conventional laboratory measurements of CEC on crushed samples. The DW papers used Q_{v_elect} for their display of the model fit to Sample 26 (Fig. 16 of Clavier et al. 1977 and Fig. 9 of Clavier et al. 1984) and suggested its use as an improvement over both WS and DW formulations. We have concluded from our study that it should be utilized and will do so for the rest of the DW model equations in the paper. We will discuss this later at Eq. (16) and the "Remedies" section.

The expression for ν_q is

$$\nu_Q = \alpha \nu_Q^H \tag{8}$$

where α is the expansion factor of the diffuse layer as pore water salinity decreases, and ν_Q^H (cm^3/meq) is the clay water volume per meq of the Outer Helmholtz plane (OHP). The value of ν_Q^H can be calculated from ionic and molecular dimensions and the slope of the specific area vs. specific CEC for clays. Clavier et al. (1977, 1984) calculated the theoretical value to be 0.28 cm^3/meq. We will be using the term $\alpha \nu_Q^H$ instead of ν_Q to explicitly illustrate the role of α for the quantification of the diffuse layer expansion. Alpha is defined as

$$\alpha = \sqrt{\frac{\gamma_l \langle n_l \rangle}{\gamma \langle n \rangle}} \tag{9}$$

where $\gamma_1 \langle n_1 \rangle$ is the NaCl activity coefficient and molarity (mol/L) respectively associated with the salinity that creates the minimum distance of the OHP. γ_1 depends on salinity and temperature and is equal to 0.71 at a molarity of 0.35 at 71.6 °F and $\langle n_l \rangle = 0.35$ independent of temperature. $\gamma \langle n \rangle$ are the values of the two constants at any other salinity and temperature. α is limited to unity at high salinities and increases as the salinity decreases below a molarity of 0.35 at 71.6 °F. ν_Q^H is a function of temperature

$$\nu_Q^H = \frac{90}{T_k} \tag{10}$$

where T_k is degrees Kelvin. At 71.6 °F, $\nu_Q^H = 0.305$. For water saturated formations and core samples examined in this analysis, Eq. 7 can be simplified and rewritten as

$$C_0 = \frac{1}{F_0}\left[\left(1 - \alpha \nu_Q^H Q_v\right) C_w + \alpha \nu_Q^H Q_v C_{cw}\right]. \tag{11}$$

Rearranging the term in brackets gives

$$C_0 = \frac{1}{F_0}\left[C_w + \alpha \nu_Q^H Q_v \left(C_{cw} - C_w\right)\right]. \tag{12}$$

It should be noted that the term $\alpha \nu_Q^H Q_v$ is the fractional volume of clay water (V_{cw}/φ_t). A value of unity for the term $\alpha \nu_Q^H Q_v$ means the clay water has filled the available pore space, displacing and excluding the pore water. This only occurs when the salinity decreases to a point where the diffuse layer is sufficiently large as determined by the terms α and Q_v. The concept of an upper bound for $\alpha \nu_Q^H Q_v$ was not previously recognized or applied by the DW authors. This has important implications where the pore water salinity is relatively fresh. We will explore this further in the "Fundamental Flaws" section.

It is convenient to write the clay water conductivity,

$$C_{cw} = \frac{\beta}{\alpha \nu_Q^H}, \tag{13}$$

where β ((S/m)/(meg/cm^3)) is the clay counterion conductivity. It has the same definition but not the same value as the *B* in the WS model. Van Olphen and Waxman (1958) experimentally found the value of β to be 1.8 for montmorillonite.

Substituting Eq. 13 into Eq. 12 gives

$$C_0 = \frac{1}{F_0}\left[\left(1 - \alpha \nu_Q^H Q_v\right) C_w + \beta Q_v\right]. \tag{14}$$

Clavier et al. (1977) found by curve fitting the measured data, that values of $\beta = 2.05$ and $\nu_Q^H = 0.305$ at 71.6 °F (22 °C), best fit the experimental data. These values are used by the DW model instead of the theoretical values discussed previously.

Unlike the WS *B*, the DW β is a function of temperature but not salinity which is explained by the fact that DW is a true parallel model. For elevated temperatures

$$\beta = 2.05 \frac{(T°C + 8.5)}{(30.5)}. \tag{15}$$

Consequently, C_{cw} only depends on temperature and the volume occupied by the clay water which is a constant at high salinity. The only free parameter for the DW formulation is the pore water salinity or conductivity; the other parameters are either dictated by electrochemistry theory or measured.

Practical Implementation for Laboratory Measurements.

The same laboratory procedures and measurements utilized for the WS formulation are used for the DW formu-

lation. Equation (15) is used to compute β for the temperature in the laboratory. Equation (10) is then used to compute v_Q^H.

When Eq. (14) is rearranged for the case of $C_0 = 0$, C_x can be solved for in terms of Q_v as $C_x = (\beta + C_x v_Q^H) Q_v$ and from this, the Q_{v_elect} is computed as

$$Q_{v\_elect} = \frac{C_x}{\beta + C_x v_Q^H}, \quad (16)$$

where C_x is the C_w or x axis intercept computed from a line drawn through the linear high salinity laboratory data where α = 1. This Q_v has been re-named Q_{v_elect} to distinguish it from the chemically derived Q_v. Because both β and v_Q^H were determined previously from the entire database using Q_{v_chem}, the computed Q_{v_elect} is not an independent variable but instead depends on the choice of β and v_Q^H . It should be thought of as a "fitting" parameter for each sample. It does improve the fit for both the WS and DW models as will be seen later. One could create a minimization routine to solve for β, v_Q^H and Q_{v_elect} simultaneously using all of the samples. We decided not to do this for several reasons. First, we wanted to maintain the use of the variable definitions and values as represented in the original WS and DW papers. Second, determining an empirical value for this group of variables would be similar to how the WS B was determined which was as a best fit for a group of samples, but not necessarily the best fit for any one sample. Third, we have developed a solution for the determination of Q_{v_elect} from electromagnetic (EM) log measurements that can be applied for each depth sample eliminating the need for determining a best fit for this variable from a group of samples. This technique is described under the "Remedies" section.

Fig. 2 illustrates the fact that Q_{v_elec} is about 50% higher than the Q_{v_chem} for the samples containing primarily illite and montmorillonite clay types. The samples with primarily kaolinite have low Q_v values but don't seem to have the same difference in Q_v values for some presently unknown reason. This requires further study.

For each measured C_0, the C_w of the saturating solution will have a unique value of α. The salinity is computed from the $C_w$value, then the activity and molarity from the salinity and temperature and finally the α value from Eq. (9). This α value is unity for Eq. (16) since only the high salinity data is used to determine Q_{v_elec}. α will increase as salinity decreases. The term $\alpha v_Q^H Q_{v\_elec}$ is then computed for use in Eqs. (11-14). The next step is to determine the cementation exponent, m, of the sample which is accomplished by a curve fitting routine using Eq. (12) through the high salinity C_0, C_w data pairs. At this point the DW forward model can be computed and plotted against the measured data.

The various components of the DW model in Eq. 12 are illustrated in Fig. 3 for Sample 26. The measured constants used in the DW model were temperature=71.6 °F (22 °C), $Q_{v\_elec} = 1.74$, $\varphi = 0.229$, $m = 2.01$ ($F_0 = 19.4$), $v_Q^H = 0.305$, $\beta = 2.05$, $\langle n_l \rangle = 0.35$, and α for each $C_w$value from Eq. (9). Fig. 3 can be compared to Fig. 9 from Clavier et al., (1984) where the same parameters are being used with the exception that our curve fit gives $Q_{v\_elec} = 1.74$, and they used $Q_{v\_elec} = 1.77$ which accounts for the slight differences. The agreement between Clavier et al. (1984) and our DW model response indicates that we have implemented the model in our software exactly as described in the paper. Fig. 16 in Clavier et al. (1977) can also be duplicated although it requires using $n_1 = 0.40$.

The black dash-dot line originating from the origin in Fig. 3 is the line representing a clean Archie type rock at the given C_w having the slope m determined by the measured data and the DW model. The difference between this line and the measured data is

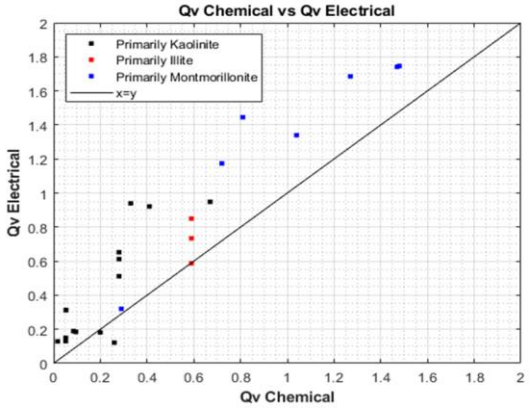

Fig. 2—Q_{v_elect} plotted vs Q_{v_chem}. There is approximately a 50% difference for the illite and montmorillonite type clays.

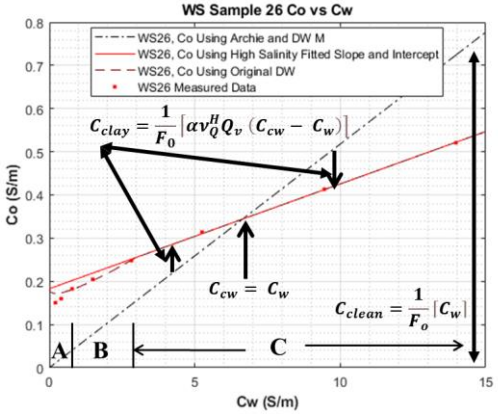

Fig. 3—DW model plotted with measured data illustrating the components of the model in Eq. 12 or 14

$$\frac{1}{F_0}\left[\alpha v_Q^H Q_v\,(C_{cw} - C_w)\right]. \quad (17)$$

Region C in Fig. 3 represents the case at room temperature where $\langle n_l \rangle > 0.35$ or C_{cw}~2.86 S/m, α is unity, C_{cw} is a constant from Eq. (13) and the model and data are linear. The difference between the terms C_{cw} and C_w determines whether the clay term adds or subtracts from the clean Archie line. When $C_{cw} = C_w$, Eq. 12 reduces to an Archie relationship and the Archie line and the DW model intersect at a value of 6.72 S/m at 71.6 °F. To the right of this intersection, $C_{cw} < C_w$, the equation on the plot is negative and the clay water can be thought of as reducing the equivalent water conductivity relative to a rock having only non-clay, pore water present. To the left of this intersection, $C_{cw} > C_w$ and the clay contribution is positive or adding conductivity relative to a clean Archie rock. The WS model as written incorrectly implies that the presence of clay will always add to the clean Archie type rock conductivity. This has caused much unnecessary confusion and led to many well-intentioned "improved" but incorrect non-parallel saturation models that were built upon the WS formulation.

In region B where $\langle n_l \rangle < 0.35$, or C_{cw}~ < 2.86 S/m, ~17,000 PPM, α increases above unity (Eq. 9). This means the fractional volume of clay water ($\alpha v_Q^H Q_v$) is no longer fixed but is increasing due to the expansion of the diffuse layer.

At the same time, C_{cw} is decreasing as computed by Eq. 13. Both effects offset each other in the term ($\alpha v_Q^H Q_v C_{cw}$) in Eq. 17, meaning the *relative* contribution of the clay water to the measured conductivity is constant. This is true for all salinities but is a unique characteristic of clay water and applies even when the diffuse layer expands. The second term in Eq. (17), ($\alpha v_Q^H Q_v C_w$) will be increasing and with the negative sign means the *relative* contribution of the pore water to the measured conductivity is decreasing. The expansion of the diffuse layer is essentially excluding an increasing portion of the connate water from the pore as C_w drops further. This causes the measured and modeled C_0 to drop below the linear high salinity trend line in region B between C_{cw}~2.86 to ~0.75 S/m. There is an additional non-linear decrease in the measured data below C_{cw}~ 0.75 S/m in region A, that is more pronounced for higher values of Q_v.

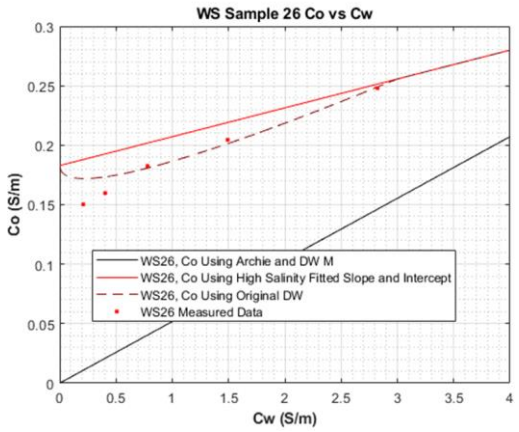

Fig. 4—DW model plotted with measured data illustrating the divergence of the model and measured data below $C_w \backsim 0.75\ S/m$ for Sample 26.

Fig. 3 illustrates that the DW model fits the data exactly at high salinity and reasonably well down to C_w ~ 0.75 S/m for Sample 26. The observation is specific for each sample and depends on the sample Q_v and clay type. Below this value the model and measured data depart from each other with the trend of the DW model curving upwards instead of downwards as the data suggests (see Fig. 4). This shortcoming will be addressed in the section "Fundamental Flaws" and a solution proposed under "Remedies". The divergence of the model relative to the data was not evident in Clavier et al. (1977, 1984, Figs. 16 and 9) respectively because they did not plot the model below a C_w of 0.2 and 0.78 S/m respectively. We added a modeled point at $C_w = 0.0001$ S/m and discovered this anomalous trend which was not disclosed by the authors.

Practical Implementation for Field Measurements.

Similar to WS, the DW model uses the parameter Q_v determined indirectly from gamma-ray, spontaneous potential or other log measurements. Spectroscopy measurements are better suited for determining $Q_v$since they offer a more accurate mineralogy determination. When using spectroscopy measurements, the bulk CEC can be computed from the summation of the individual clay mineral dry weight volumes times their respective CEC values. Equation 2 is then used to compute the formation Q_v.

The cementation exponent found using the DW formulation has been found to be approximately 2 regardless of shale type or volume (Clavier et al. 1977, 1984). At 71.6 °F, C_{cw} is 6.72 and increases with temperature due to both α and v_Q^H changing with temperature Eqs. (9,10). Only the inputs of Q_v and C_w needed to compute S_{wt} from Eq. (7).

Improvements Brought by the DW Model

The DW Model Presents Clay and Pore Water Conductivities in a True Parallel Conductivity Model

The 1984 version of Clavier et al. put their model at the beginning of the paper. Their Eq. (1) is the basis of the model, $C_t = [(S_{wT})^n/F_0]\, C_{we}$. This is the Archie model with a modified brine conductivity, C_{we}. Their Eq. (2) is $V_{cw} = \alpha v_Q^H Q_v \varphi_t$. By conventional definition, φ_t (the porosity) is the fraction of the total volume that is void space. The quantity $\alpha v_Q^H Q_v$ is the fractional volume of the pore space occupied by the clay water. V_{cw} is then the volume occupied by the clay water. S_{wT} is the total fractional water volume which includes the non-clay and clay water.

Therefore, $0 \le V_{cw} \le \varphi_t$. This requires that $0 \le \alpha v_Q^H Q_v \le 1$ when $S_{wT} = 1$ as discussed earlier.

Their Eq. (3) is for the volume of the "far water" (or "free water").

$$V_{fw} = V_w - V_{cw} = \varphi_t\left(S_{wT} - \alpha v_Q^H Q_v\right) \qquad (18)$$

The limiting values of V_{fw} are 0 and $\varphi_t S_{wT}$; i.e., $0 \le V_{fw} \le \varphi_t S_{wT}$. Since $V_{fw} \ge 0$, the $\alpha v_Q^H Q_v$ term is required to be between the limits of $0 \le \alpha v_Q^H Q_v \le S_{wT}$.

The equivalent water conductivity,

$$C_{we} = \frac{(S_{wT} - \alpha v_Q^H Q_v) C_w + \alpha v_Q^H Q_v C_{cw}}{S_{wT}} \qquad (19)$$

is written more transparently as

$$C_{we} = \left(1 - \frac{\alpha v_Q^H Q_v}{S_{wT}}\right) C_w + \frac{\alpha v_Q^H Q_v}{S_{wT}} C_{cw}. \qquad (20)$$

This is clearly a volume-weighted average; the coefficients in front of C_w and C_{cw} add to 1, and the fractional volumes referred to are separate volumes. We saw previously that $0 \le \alpha v_Q^H Q_v \le S_{wT}$, so that $0 \le \frac{\alpha v_Q^H Q_v}{S_{wT}} \le 1$, the lower limit occurs when the clay volume is zero, and the upper limit occurs when the pore volume that is not occupied with hydrocarbons is occupied by clay water.

DW Model Proves That the Cementation Exponent Does Not Increase with Shaliness

As mentioned previously, the cementation exponent, m, of the sample is determined by a curve fitting routine using Eq. (11, 12 or 14) and the high salinity C_0, C_w data pairs. The resulting m_{DW} for the 27 samples from WS 1968 are shown in Fig. 5. The m does not increase with shaliness but instead is approximately two. The kaolinitic samples have a lower m value but the low clay volumes may preclude any conclusions about how their cementation exponents would behave at higher clay volumes of kaolinite.

The reason the cementation exponents computed using the WS model increase with shaliness is because the WS model fails to account for the fractional volumes of clay vs. pore water in the formation. This results in the WS model not being a truly parallel conductivity model. This is discussed in more detail in Appendix A.

B Is Correctly Characterized as a Theoretical Value and Does not Change with Salinity Down To ~1 S/m

The Waxman-Smits value for the equivalent conductivity of the compensating counterions, *B*, changes with salinity (C_w) and temperature. The change with salinity is due to WS not accounting for the fractional volumes of the clay and pore water. By accounting for these volumes, the DW model is able to use a *B* value that is only dependent on temperature and in the same range as the value of 1.8 determined by Van Olphen and Waxman (1958) for suspensions of sodium bentonite (montmorillonite) and water.

DW Model Accounts for the Measured Temperature Effect on B

Clavier et al., (1977, p 10) explain that v_Q^H will decrease with temperature. This will be the cause of the increase of the slope of the C_w vs. C_0 crossplot at high salinity as temperature increases. Reinterpreting the data from Waxman and Thomas (1974), Clavier et al. (1977) determined that β changes with temperature but not salinity.

DW Model Accounts for the Curvature of the $Q_{v\_}$ vs. C_x Crossplot of WS

A plot of Q_{v_chem} vs. C_x shows a slight curvature in the relationship. WS placed a linear equation through this data which required that *B* was independent of clay type and counterion concentration. In fact, Q_{v_chem} *vs* C_x is

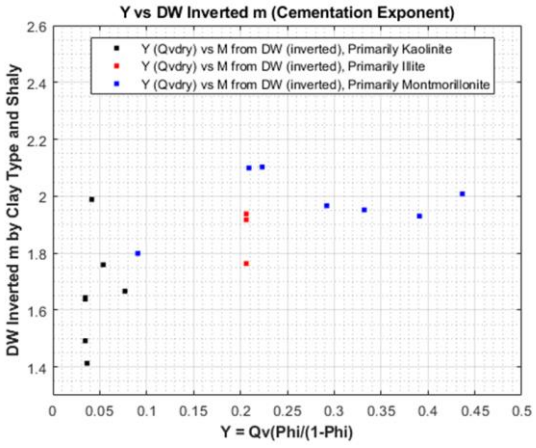

Fig. 5—DW inverted m using Eq. 12 and the measured data. Y is Qv on a dry rock basis.

not a linear relationship but is non-linear according to the formula

$$C_x = \frac{\beta\, Q_{v\_chem}}{1 - v_Q^H\, Q_{v\_chem}}. \quad (21)$$

Clavier et al. (1977) found that the values of $B = 2.05$ and $v_Q^H = 0.28$ in the non-linear Eq. 21 best fit the data.

There Are No Parameters that Need Manipulation When Analyzing Core Measurements Above Cw=1 S/m

All of the parameters of the DW model are determined from the laboratory conductivity measurements taken at multiple salinities on the core as explained under the section "Review of DW Theory". For log measurements, the pore water salinity is a necessary input. The value of C_{cw} is computed from Eq. 13 and is dependent only on temperature which affects v_Q^H. The input of pore water salinity requires a computation of α.

FUNDAMENTAL FLAWS OF THE SHALY SAND MODELS

Waxman-Smits Model

WS is not a Parallel Conductivity Model

Waxman-Smits write in their Eq. (2) $C_0 = xC_e + yC_w$. It is a mixing rule for two non-zero conductivity values. They claim it is a parallel conductivity model. It *could* be a parallel conductivity model, but only if x and y are chosen to make this so. In conductivity terms, $C_0 = yC_w$ is one possibility. For this to happen, x must be zero. In this case if y is chosen so that $y = \varphi^m$, then the model reduces to Archie's model. This tells us that y is a function of porosity. If all the Cs have the same units, then x has the same units as y and must also be a function of porosity. Another possible value for C_0 is $C_0 = xC_e$. By analogy with the Archie model, then $x = \varphi^m$. In the case where $x = 0$ or $y = 0$ then φ is the entire pore volume. Otherwise, the pore space is shared between C_e and C_w. The simplest method to partition the pore volume is $\varphi_t = \varphi_e + \varphi_w$. Then $\varphi_w = \varphi_t - \varphi_e$. So, $C_0 = \varphi_e^{m_e} C_e + (\varphi_t - \varphi_e)^{m_w} C_w$. This is a volume-weighted average.

To see this more clearly, write the equation factored as $C_0 = \varphi_e \varphi_e^{m_e - 1} C_e + (\varphi_t - \varphi_e)(\varphi_t - \varphi_e)^{m_w - 1} C_w$. The red text, ($\varphi_e$ and $(\varphi_t - \varphi_e)$), indicates the volume weighting. The terms $\varphi_e^{m_e - 1}$ and $(\varphi_t - \varphi_e)^{m_w - 1}$ are geometrical factors, with m_e potentially (and probably) not equal to m_w.

According to the analysis above, $x = \varphi_e^{m_e}$ and $y = (\varphi_t - \varphi_e)^{m_w}$. This is NOT the Waxman-Smits model. Why? Because in their Eq. (3) they set $x = y$. This would require that $m_e = m_w$ and $\varphi_w = \varphi_t - \varphi_e$. And this requires that $\varphi_w = \varphi_e = \varphi_t/2$. Putting all this together, $x = y = (\varphi_t/2)^m$ and

$$C_0 = \left(\frac{\varphi_t}{2}\right)^m (C_e + C_w) \ldots$$
$$\approx \frac{\varphi_t^m}{4}(C_e + C_w) \neq \varphi_t^m (C_e + C_w) \quad (22)$$

Waxman and Smits just *assert* $x = y = 1/F^* = \varphi^{m^*}$. The way they make this happen is to *not* partition the pore space. In other words, C_e and C_w are put into the same pore space. This is seemingly nonsensical, and only makes sense if C_e and C_w were expressed in terms of concentrations instead of conductivities. You can easily imagine a volume, say a tube, and then vary the concentration of potassium in the tube without affecting a concentration of sodium in the same tube, and vice versa. Nothing changes if the potassium is replaced by sodium, so that two separate sodium concentrations are under consideration, one for brine and the other for the clay counterions. We explain the requirements for a parallel model in more detail in Appendix A.

Apparent Formation Factor and Corresponding Cementation Exponent Increase with Shaliness.

The dash-dot black line in Fig. 3 represents the formation factor and associated cementation exponent which satisfies the DW model. This cementation exponent is 2.01. The formation factor is the inverse of the slope of this line. A lower slope represents a larger formation factor and higher cementation exponent. The measured data exhibits an apparent slope (red solid line) that is lower than the slope determined from using the DW formulation. The reason for the difference between the two lines is described by the equations shown on the plot. At high salinity where $C_{cw} < C_w$, the term $(C_{cw} - C_w)$ is negative and the clay water is causing the C_0 to be less than that expected from an Archie formulation. When $C_{cw} > C_w$ the term $(C_{cw} - C_w)$ is positive and the clay water is causing the C_0 to be greater than that expected from an Archie formulation. The DW formulation provides the proper quantification of the response of the clay water to the measured conductivities and shows that the cementation exponent does not increase with clay volume. See Fig. 5 for quantification.

WS Equivalent Counterion Conductance (B) Varies with Salinity and Q_v.

The Waxman-Smits value of B varies with salinity, Q_v and temperature while the variable, β, in the DW model varies only with temperature (Eq. 15). The WS B is strictly an empirical parameter used with F^* and Q_v to quantify the difference between the black dashed and black dash-dot lines in Fig. 1. Because F^* and Q_v are constants, B necessarily must vary with salinity as illustrated in the equation for the clay conductivity shown between these two lines in Fig. 1. We know from the parallel DW model that the change in slope of the measured

data from C_{cw}~2.86 to ~1 S/m at room temperature is due to the expansion of the diffuse layer and not a change in B with salinity. The additional decrease in equivalent counterion conductivity below C_{cw} ~1 S/m is discussed under the "Remedies" section.

The change in WS B with Q_v for the high salinity measurements is documented and discussed in Clavier et al., (1977). By equating the terms from the WS and DW models at high salinity where α = 1,

$$WS\ B = \frac{DW\ \beta}{1 - v_Q^H Q_v}. \quad (23)$$

This equation illustrates that as Q_v increases, the WS B will necessarily increase.

WS Model Does Not Fit the Measured Data Very Well Especially at the Low Salinities.

The Waxman-Smits model was found to have errors between the modeled C_o and the measured C_{cw} at both high and low salinities, with somewhat greater error at the low salinities. This is because the WS B is required to account for not only the clay counterion conductivity but also the multiple effects of the lack of a parallel model in a parallel conductivity system, the expansion of the diffuse layer, and the "apparent" changing slope or formation factor with shaliness and salinity. Fig. 6 shows the data and model fit for Sample 23 which has the best fit of the shaly cores from the 27 samples. Fig. 7 shows the fit for Sample 26 which has about the average discrepancies. Table 1 compares the "goodness-of-fit" for the various WS models described in the next section as well as the various DW models studied in this paper that will be discussed later.

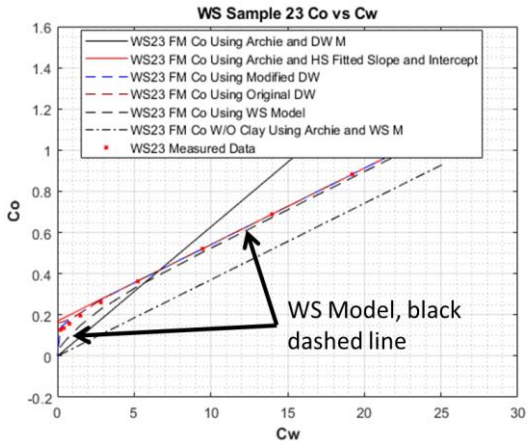

Fig. 6—C_o vs C_w for WS Sample 23 which has $Q_v = 1.04$. This core exhibits the best fit for the WS model for the shaly cores from the WS Table 7 database.

The WS Parameter B, Has Been Modified Through the Years, Creating a Worse Fit to the Data.

We have found three different equations in the literature for the WS B term. First was the original formula in Waxman-Smits, 1968 given as

$$B_{1968} = 4.6(1 - 0.6e^{-0.77 * C_w}). \quad (24)$$

A modification to this formula was published by Waxman and Thomas (1974)

$$B_{1974} = 3.83(1 - 0.83e^{-0.50 * C_w}) \quad (25)$$

Juhasz (1981) published another equation

$$B_{1981} = \frac{-1.28 + 0.225 * T - 0.0004059 * T^2}{1 + R_W^{1.23}(0.045 * T - 0.27)}, \quad (26)$$

and finally, Waxman, Thomas (2007) published an updated chart for elevated temperatures without an equation but apparently, from looking at the chart, used the same equation at 25 °C as in 1974.

$$B_{2007} = 3.83(1 - 0.83e^{-0.50 * C_w}) \quad (27)$$

The WS model using all three equations for B are plotted in Fig. 7. For Sample 26, the best fit to the measured data is provided by the original equation provided by Waxman-Smits (1968).

Columns A-C in Table 1 list the "goodness-of-fit" of the WS models using the various formulas for B shown in Fig. 7 for all 27 samples using Eqs. 24-26 and Q_{v_chem} as is the normal practice in the industry.

The "goodness-of-fit" is computed as

$$Var = \frac{\sum (C_{o\_modeled} - C_{o\_measured})^2}{238}. \quad (28)$$

The best fit to the measured data is achieved by using the original B proposed by Waxman-Smits 1968. We did not

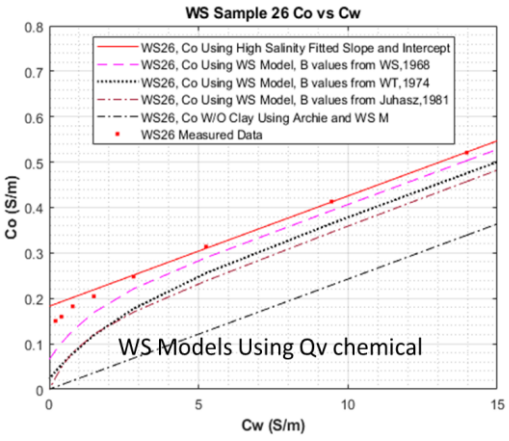

Fig. 7—C_o vs C_w for WS Sample 26. The WS model using the various published equations for B listed in the legend. The original equation from Waxman-Smits in 1968 fits Sample 26 better than the later modified equations.

compute the "goodness-of-fit" for other data sets having saturations less than unity.

Dual Water Model

The term $\alpha v_Q^H Q_v$ was not limited to $0 \le \alpha v_Q^H Q_v \le S_{wT}$.

The Dual Water model as published in Clavier et al. (1977, 1984) did not mention the need to place limits on the quantity $\alpha v_Q^H Q_v$. From Eq. (18), $\left(S_{wT} - \alpha v_Q^H Q_v\right)$ is the total fractional volume of water minus the clay water fractional volume. This difference in the parenthesis is then the fractional volume of non-clay water associated with C_w. Physically, this non-clay water fractional volume cannot be less than zero. We also know that $\alpha v_Q^H Q_v$ must be greater than zero. In all petrophysical models for saturation, the assumption is that the hydrocarbons displace only the non-clay water. The lowest non-clay water fractional volume is therefore zero meaning that the clay water fraction can be equal to S_{wT} but not exceed S_{wT}.

Therefore, the term $\alpha v_Q^H Q_v$ is required to be between the limits of

$$0 \le \alpha v_Q^H Q_v \le S_{wT}. \tag{29}$$

An Analytical Method to Convert Salinity to C_w at a Given Temperature is not Presented.

Petrophysical relationships require a method to convert from water salinity to conductivity at any given temperature and vice versa. When the DW model was implemented into certain well known multi-mineral petrophysical software packages circa 1987, a new method to compute salinity from water conductivity and vice-versa was invented but never published or patented. SLB has decided to keep the algorithms a trade secret. Previous historical algorithms do not fit the International Critical Tables of Numerical Data (ICT, (NRC, 1933) data over the entire range of applicable temperatures and salinities. The new algorithm fits both the ICT data as well as the in-house data measured by Scala over the temperature range of 32-400 °F and a salinity range of 0-260 PPK with an accuracy of ±2%.

The SLB chartbook Gen-9 where salinity and water resistivity are plotted as a function of temperature has not been updated with this new algorithm. Differences will be found mainly at the higher temperatures for all salinities. The conversion from salinity to conductivity and vice versa also makes use of a new, more accurate algorithm to compute the NaCl activity coefficient.

A Method to Compute NaCl Activity Coefficient and Molarity from Temperature and Salinity is Not Presented.

The computation of the NaCl activity coefficient is a trade secret. However, Truesdell (1968) has published a table of the NaCl activity coefficients for molarities from 0 to 1 mol/L and from 15 to 50 °C. Truesdell's work, and references show that the NaCl activity coefficient is unity at 0 mol/L, decreasing to a minimum value at about 1 mol/L and gradually increasing as molarity increases.

Fortunately, the calculation of molarity is a well-known computation in the chemical industry. These two constants are key to the calculation of α in Eq. (9).

Molarity for use in the DW model is

$$molarity = \frac{PPK\ \rho_{sw}}{58.45}, \tag{30}$$

where PPK is the salinity in parts per thousand and ρ_{sw} is the density of the salt and water mixture.

Fundamental Flaws of Both Models

Poor Fit to Low Salinity Data.

We explained previously that there are conditions at low salinity where the diffuse layer has expanded such that the clay water occupies the entire pore space. When the salinity is lowered further, there is a change in the C_0 response that is not captured by the published DW model or electrochemistry theory. This results in the poor fit of the DW model to the measured data at low salinities for shaly sands (Fig. 8). Clavier et al. (1977, 1984) acknowledged this characteristic of their fit even with the erroneously unlimited values of α as demonstrated in Fig. 3. Clavier et al. (1977) quote

> The additional drop of C_0 below 1 S/m must be attributed to other causes, probably the decrease in counterion mobility in dilute solution as suggested by Waxman (1968), and van Olphen, Waxman (1958).

Clavier et al. (1977) suggested the use of a dilution factor for *B*, but never put it into practice. Had they correctly used a limited α (Fig. 8) instead of an unlimited α, and

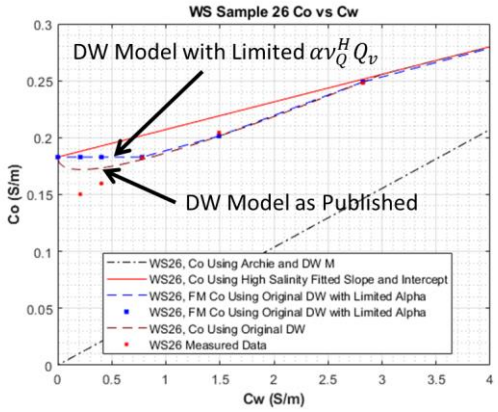

Fig. 8 - DW model plotted with measured data using a limited value of α (blue dashed line) and $\alpha v_Q^H Q_v$. The original, as published DW model is brown dashed line. Below $C_w \sim 0.8$ for Sample 26, the correctly limited α DW model produces a constant C_0 response and worse fit to the data.

noticed the poor fit, they most likely would have published and developed the DW model with this dilution factor.

Waxman-Smits (1968) empirically capture this additional counterion mobility decrease by decreasing their *B* more dramatically as salinity decreases. The trend of the WS model looks reasonable although the absolute value is incorrect in cases like Sample 26, shown in Fig. 7.

The response of the DW model with a correctly limited α, Fig. 8, clearly shows the need for a dilution factor.

We reason that as the diffuse layer expands, there comes a point where the hydrated counterions are so far removed from the clay surface that they are no longer influenced by it. These counterions and their properties become indistinguishable from the hydrated cations in the pore water causing the clay water conductivity to become more and more equivalent to the pore water conductivity.

We have developed our own function for the dilution factor, and this is explained under the "Remedies" section.

Q_{v_elec} is Needed to Improve the fit for Both WS and DW Models

We previously mentioned the use of Q_{v_elec} with the DW model and the fact that we use it for all of the DW models we have analyzed. Equation 16 gives the formula. We also tried using the same Q_{v_elec} values in the WS models. This results in a better fit for the WS models. Figure 9 illustrates this improved fit of the WS models to the measured data from their Table 7. The improved "goodness-of-fit" for the WS model using the 1974 value of *B* and Q_{v_elec} (column D) instead of Q_{v_chem} (column B) is shown in Table 1.

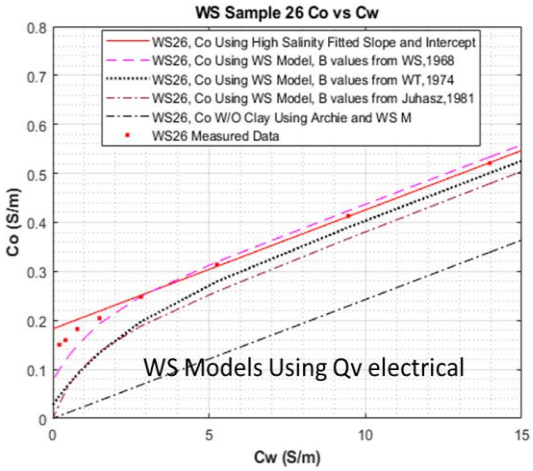

Fig. 9—C_0 vs C_w for WS Sample 26. The WS model using the various published equations for B listed in the legend. Q_{v_elec} has been used instead of Q_{v_chem} which improves the fit. Compare to Fig. 7

We tested the use of Q_{v_chem} instead of Q_{v_elec} in the DW model. The "goodness-of-fit" worsens by a factor of ten as shown in Table 1, columns G vs. H.

WS B and DW β Assume a Single Species of Cation is Present in the Laboratory Environment While Multiple Species of Cations are Present Downhole.

The electrical double layer consists of the adsorbed water, the hydrated cations within the outer Helmholtz plane, and the exponential decaying concentration of cations in the diffuse layer that decay as a function of distance from the outer Helmholtz plane. There is also an increasing concentration of the excluded anions in the diffuse layer as a function of distance from the outer Helmholtz plane. The "Electrochemistry" section of Appendix A explains the concept of molar conductivities and how each species of both cations and anions will uniquely contribute to the conductivity of the mixture.

The WS model models the equivalent clay cation conductivity, B, as a function of the properties of only the sodium cation and then determines the high salinity value empirically from C_x using Q_{v_chem}. The DW model validates their experimentally derived value of β to laboratory measurements of the sodium cation molar conductivities in montmorillonite slurries. The equations for both models assume that only one species of cation is present and compute its apparent molar conductivity from the measured laboratory data.

The laboratory CEC measurement reflects the positive equivalents needed to satisfy the clay surface charge. Any anions present in the diffuse layer are not measured with a CEC measurement. For laboratory data flooded with NaCl solutions, it would make sense to use a chemically derived CEC in the equations. However, we see that Q_{v_elec} is higher than Q_{v_chem} computed from the laboratory CEC. This could be due to errors in the values of Q_{v_chem} that are derived from CEC measurements. It could be from any anions present in the clay water. It could also be that Q_{v_chem} is correct, but B or β is incorrect due to 1) unmeasured anions and possibly differing dissolved cations in the equilibrating fluid for each sample are varying, and 2) using a model that assumes only one species of cation is present is unable to properly determine the value of B or β that is actually varying per sample. When we use Eq. (16) to compute Q_{v_elec}, it could be that B or β is varying per sample instead of Q_v.

Further complications occur downhole. In the downhole environment, cations attached to the clay surface can include sodium, potassium, calcium, magnesium, and others. (See Appendix A for the equivalents associated with various cations). These various cations all have different mobilities and molar conductivities. At low salinities, the

excluded anions in the diffuse layer will be present. This may cause the WS B and DW β to have even different values downhole than those determined in the laboratory.

We could have chosen to calculate β, or Q_{v_elec} or their product from C_x. Since β changes with temperature and Q_v does not, we chose to compute Q_{v_elec} from the laboratory data to eliminate confusion when comparing variables. We follow the same convention when computing a Q_{v_elec} from log measurements downhole as explained under "Remedies".

MODEL REMEDIES

We focus on the solutions found for the flaws in the DW model since the DW model has been found to remedy the primary flaws found in the WS model.

Limiting α and $\alpha v_Q^H Q_v$ at Low Salinity.

We previously discussed the fact that for the water saturated samples measured at room temperature, $\alpha v_Q^H Q_v$ does indeed exceed a value of S_{wT} or unity at the lowermost salinities due to the expansion of the diffuse layer. We will now discuss how we have implemented this upper limit and the consequences of doing so.

The term α depends only on salinity, starting at unity, then increasing as the salinity decreases as illustrated in Table 2. The term v_Q^H, is constant at constant temperature and the term Q_v varies with each sample. Therefore, the salinity at which $\alpha v_Q^H Q_v$ exceeds S_{wT}, or unity for our cases, varies with each sample. We have computed the values of $\alpha v_Q^H Q_v$ for each sample at each salinity. When $\alpha v_Q^H Q_v$ exceeds S_{wT}, which is when the volume of clay water fills the available pore space, we limit $\alpha v_Q^H Q_v$ to S_{wT}. We then compute the maximum allowed α as $\alpha_{limited} = \left(\alpha v_Q^H Q_v\right)_{limited} / v_Q^H Q_v$ for use in the equations where α appears, starting with Eqs. (7, 11).

Table 3 lists the limited α for each sample at each salinity for $S_{wT} = 1$ and 71.6 °F. Because the term $\alpha v_Q^H Q_v$ will exceed $S_{wT} = 1$ sooner for higher values of Q_v at any given pore water salinity or C_w, the limited α will depend on both salinity and Q_v.

Table 4 shows the corresponding values of $\left(\alpha v_Q^H Q_v\right)_{limited}$ for $S_{wT} = 1$ for the laboratory measurements for reference.

When α is limited to the maximum allowed value at the lower salinities, the term C_{cw}, Eq. (13), becomes constant. This causes the right-hand term inside the brackets in Eq. (11) to be a constant. The left-hand term is zero since $\alpha v_Q^H Q_v$ has been limited to S_{wT} or unity in the case for the water saturated laboratory measurements. Figure 8 shows the DW model results for both the original model as published and the limited α model. Table 1, columns E and F show the "goodness-of-fit" for both models. The limited α model does not fit the data as well as the unlimited model and it is obvious from Fig. 8 that the majority of the misfit occurs at the lower C_w values.

The term volume $\alpha v_Q^H Q_v$ is referred to as the clay water or bound water saturation (S_{wb}) within SLB training documents. When SLB implemented the DW model into software packages they realized that S_{bw} should be limited to $S_{bw} \le S_{wt}$ just as we have done. Therefore, the Schlumberger petrophysical packages for the DW model are using the "limited" model we display in Fig. 8. It would be very difficult to match downhole water saturations in fresh-water shaly reservoirs using the commercial software packages. When reservoirs with low clay volumes have sufficiently high salinities there should not be a problem in meeting the criteria $S_{bw} \le S_{wt}$. However, as the shale content and temperature increases, this condition may not be met as discussed next.

Sample 26 has a clay fraction of 100% montmorillonite or smectite as shown in the header of Table 2. Using the values in the header and $\rho_{dcl} = 2.65$, $CEC_{dcl} = 0.90$, $Q_{v\_elec} = 1.74$ and the relationship

$$Q_v = \frac{V_{dcl}\, CEC_{dcl}\, \rho_{dcl}}{\varphi_t}. \quad (31)$$

we can compute the volume of dry clay in Sample 26 as 17%. This is not an overly shaly sand. For shalier sands and shales, we would expect the α to be limited at proportionately higher values of C_w. The effect of increasing Q_v can be seen by comparing sample 26 to Sample 22. When Q_v has doubled, the value of C_w at which $\alpha v_Q^H Q_v$ is limited has increased by a factor of 3.7, from 0.21 to 0.78.

To illustrate realistic reservoir conditions, the effect of increasing temperature to 150 °F and lowering saturation to 0.50 is shown in Table 5. Increasing the temperature to 150 °F decreases v_Q^H from 0.305 to 0.266, a 13% decrease Eq. (10). This is more than offset by the 75% decrease in saturation. The result is that $\alpha v_Q^H Q_v$ is being limited at progressively higher salinities for more of the samples.

In Table 4, the minimum $\alpha v_Q^H Q_v$ for Sample 26 is 0.53 at high salinity. In Table 5, the minimum $\alpha v_Q^H Q_v$ decreases to 0.46 at 150 °. This means the fractional volume available for hydrocarbons is (1-0.46) or 0.54. Therefore, when we set $S_{wt} = 0.5$, there is room for the hydrocarbons. As α increases at low salinities, the additional fractional volume taken up by the clay water excludes more and more hydrocarbons from the pore space. This is shown by the limited value of 0.50 in the shaded area of the table. When we further decrease $S_{wt}$to 0.25

at 150 °F in Table 6, the limits are reached for even higher salinities for more samples. When considered from a geological perspective, this means that it is physically impossible to fill the available space with hydrocarbons since it is occupied by the clay water.

It is obvious that limiting $0 \le \alpha v_Q^H Q_v \le S_{wT}$ is required for shaly formations at downhole temperatures. This is a volumetric consideration independent of the modeled or measured conductivity. However, when $\alpha v_Q^H Q_v$ is limited, the modeled conductivity using Eq. 11, 12 or 14 does not fit the measured conductivity as shown in Fig. 8. We provide a solution in the next section.

Dual Water Model Adjustments to Adjust β to Fit the Low Salinity Data.

We have determined the trend of the difference between the measured C_0 and modeled C_0 using the limited $\alpha v_Q^H Q_v$ fits a logarithmic trend as a function of C_w. There also seems to be a difference in this trend between the kaolinite- and montmorillonite-rich samples.

There are not enough samples to determine if there is a separate trend for illite and chlorite rich shales (the volume percentages of the clay fraction are given in the header of Table 2). We have therefore chosen to combine the volume fractions of kaolinite, chlorite and illite together while keeping montmorillonite as a separate volume. We did this based on a consideration of similar CEC values for kaolinite, chlorite and illite vs. montmorillonite.

The volume fraction of montmorillonite is

$$V_{f\_mont} = \frac{V_{mont}}{V_{clay}}, \tag{32}$$

with the volume fraction of non-montmorillonite clay being:

$$V_{f\_non\_mont} = \frac{V_{kaolinite} + V_{illite} + V_{chlorite}}{V_{clay}} \tag{33}$$

We further define fitting coefficients as

$$C_{w\_B\_coeff} = \left(-0.05V_{f_{mont}} + 0.15\right) \text{ and} \tag{34}$$

$$C_{w\_B\_constant} = \left(0.05V_{f_{mont}} + 0.95\right). \tag{35}$$

Then we define the ratio of B to $B_{diluted}$:

$$B_{ratio} = C_{w\_B\_coeff} Ln(C_w) + C_{w\_B\_constant}. \tag{36}$$

From this, $B_{diluted}$ can be computed as

$$B_{diluted} = B \times B_{ratio} \tag{37}$$

and used in place of B in the DW C_0 equations.

The result of applying $B_{diluted}$ is shown in Fig. 10 for Sample 26. This results in an improved fit to the data below $C_w < \sim 1$. The improvement in the "goodness-of-fit" is a factor of 3.4 and shown in Table 1, columns F and G.

Computation of Cementation Exponent from Core Measurements.

The conventional method of determining cementation exponents from core data utilizes the formation factor plot. However, before data can be plotted on this plot a shale correction must be made. For both the WS and DW methods a cementation exponent needs to be computed before the shale correction can be made creating a dilemma. Fig. 11 is a plot of the 27 samples for each salinity along with the cementation exponents 1 through 3. This illustrates that the derived cementation exponent from this plot will depend not only on the shaliness but also depend on the pore water salinity at which the conductivities were measured. Figs. 12-14 illustrate the trend of increasing cementation exponent with increasing pore water salinity by clay type. Notice how the

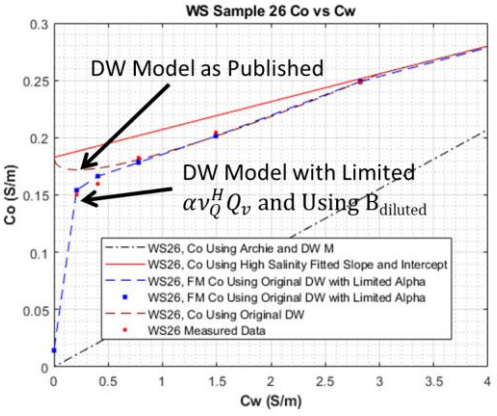

Fig. 10 - DW model plotted with measured data using the necessary limited value of α and the $B_{diluted}$ computed in Eq. 36-37.

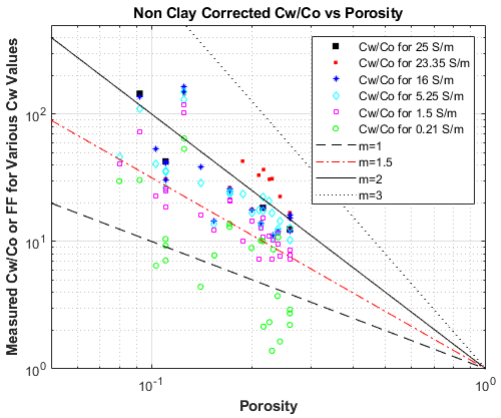

Fig. 11—Formation Factor plot for all 27 samples from WS Table 7 data showing how both salinity and shaliness affects the apparent cementation exponent when using this plot.

cleaner samples in the database move relatively little due to their low clay content.

When there is no clay present in a sample, the Archie relationship is valid, and all the data points fall on one line through the origin of a C_w vs. C_0 plot. All salinities have the same C_w/C_0 ratio for the various values of C_w. Therefore, the multiple data points on the C_w vs. C_0 plot would plot as one point on the formation factor plot for that sample. When clay is present, each point has a different "apparent" cementation exponent on the C_w vs. C_0 plot because the C_w/C_0 ratio increases with salinity (C_0/C_w decreases with salinity). This causes the multiple data points on the C_w vs. C_0 plot to move vertically on the formation factor plot as salinity increases. This is illustrated in Figs. 12-14 by observing how the shalier sample points migrate up on the formation factor plot as the plotted salinity increases. Therefore, the apparent cementation exponent increases with salinity.

Increasing clay volume has the opposite effect compared to salinity. The C_w/C_0 ratio decreases as clay volume increases for any given salinity. For any given sample porosity and salinity, adding clay would cause the data to move down on the formation factor plot, therefore decreasing its apparent cementation exponent. Figs. 11-14 illustrate the futility in determining cementation exponents from a formation factor plot.

We previously mentioned the calculation of the DW cementation exponent for each sample under the section "Review of DW theory". Essentially Eqs. 11, 12 or 14 can be used in a linear regression routine to determine the cementation exponent for each sample using the measured data at the various salinities. Obviously, the term $1/F$ is transformed to φ^m.The use of the limited $\alpha v_Q^H Q_v$ and $B_{diluted}$ may also be used but is not required.

To simplify the process and increase the accuracy we use only the high salinity data where these two variables are not required to be limited or altered as they need to be for the low salinity data. We find that the high salinity data always forms a linear trend, and the determination of the cementation exponent is robust. Fig. 5 shows the results and illustrates that when using the DW model, the cementation exponent does not change with salinity, clay type, nor clay volume as a cementation exponent derived from a formation factor plot would do.

A standard practice in the laboratory is to flood the core sample with the same salinity water as the reservoir. We previously discussed how the apparent cementation exponent changes with salinity. However, there is one salinity that can be used that will represent the true cementation exponent and the one to use in the DW models.

The calculation of the cementation exponent to use with

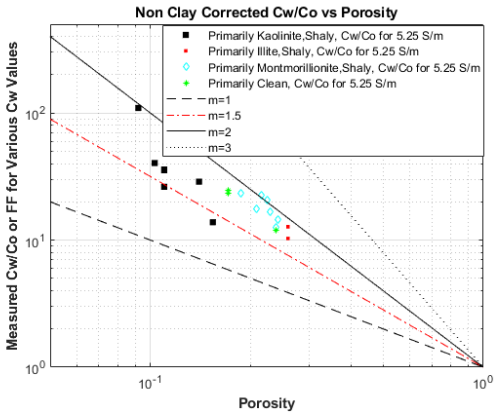

Fig. 13—Formation Factor plot for all 27 samples from WS Table 7 data at C_w=5.25 S/m. Both salinity and shaliness affect the apparent cementation exponent when using this plot.

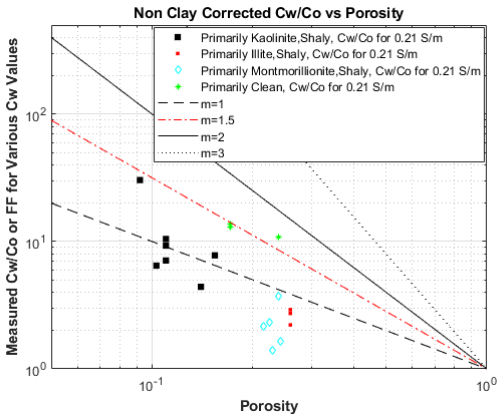

Fig. 12—Formation Factor plot for all 27 samples from WS Table 7 data at C_w=0.21 S/m. Both salinity and shaliness affect the apparent cementation exponent when using this plot.

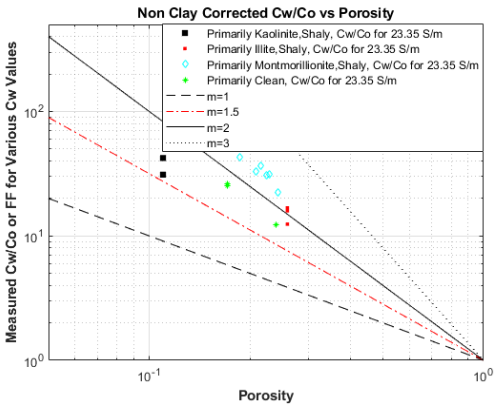

Fig. 14—Formation Factor plot for all 27 samples from WS Table 7 data at C_w=23.35 S/m. Both salinity and shaliness affect the apparent cementation exponent when using this plot.

the DW model is found by recognizing that when $C_w = C_{cw}$, the DW model reduces to an Archie model as shown in Eqs. (7,11). This is illustrated graphically in Fig. 3. Eq. 13 shows that the value of C_{cw} is fixed at 6.72 S/m at 71.6 °F. By flooding the core with this value of C_w, only one measurement of C_0 needs to be taken to determine the cementation for each sample to use in the DW model. This would save time and resources but would eliminate the ability to compute Q_{v_elec} using the multiple high salinity measurements. This is not an issue if the implementation of determining Q_{v_elec} from in-phase and quadrature log measurements is implemented as discussed in the "Remedies" section.

Q_{v_elec} is a "Fitting" Parameter and is Higher Than Q_{v_chem}.

We discussed the necessity of using Q_{v_elec} to improve the "goodness-of-fit" for both the WS and DW models. The correlation between Q_{v_elec} and Q_{v_chem} is not well defined (Fig. 2). Clavier et al. (1984) found Q_{v_elec} to be elevated over Q_{v_chem} by an average of 22% when analyzing the measurements from Waxman Thomas (1974). We have an average increase of 50% when analyzing the Table 7 samples from Waxman-Smits (1968). This makes the use of Q_{v_chem} in shaly sand models questionable.

We have recently invented a method of determining Q_{v_elec} from downhole log measurements by incorporating the quadrature conductivity from low frequency EM laterolog, propagation and/or induction measurements and is discussed next.

Computation of Q_{v_elec} using Both Real and Quadrature Conductivities Simultaneously.

Vinegar and Waxman (1984) measured the complex conductivity of cores from 3-1000 Hz to study the effect of clays on the out-of-phase or quadrature conductivity. Revil (2012) developed a petrophysical model equation to interpret this quadrature conductivity using

$$\sigma_x = -\frac{2}{3}\beta_+^s f \rho_g S_{wt}^{n^*-1} CEC \qquad (38)$$

where CEC and Q_v are related through Eq. (2), β_+^s is the counterion mobility in the Stern layer, f is the fraction of the counterions in the Stern layer compared to the total counterions and ρ_g is the sample grain density. Figure 15 shows the modeled and measured quadrature conductivities for the four samples measured by Vinegar and Waxman (1984).

Of particular interest is the fact that the quadrature conductivity is relatively independent of salinity until C_w drops below ~1 S/m, similar to the value where the in-phase conductivity drops and where the $B_{diluted}$ term was needed. This drop also happens at higher values of C_w for sample 3323C that contains primarily montmorillonite. We theorize that the decrease in the counterion conductivity is affecting both in-phase and quadrature conductivities. A better quantification of this effect will be determined from further analysis of laboratory multi-frequency measurements of synthetic clay and glass bead mixtures.

Equation (38) can be used with Eq. (7) to simultaneously solve for both the CEC and salinity of the pore water using a minimization routine. Fig. 16 illustrates the ability of the inversion to match the measured *CEC* values. The inversion was performed for two values of C_w, 4.68 and 8.6 S/m.

There are generally three primary unknowns for shaly sand analysis. They are S_w, C_w, and CEC or Q_v. Having two equations allow us to solve for any two out of the three unknowns simultaneously. For Fig. 16 we also solved for S_w which is plotted in Fig. 17. The accuracy of the inversion is remarkable.

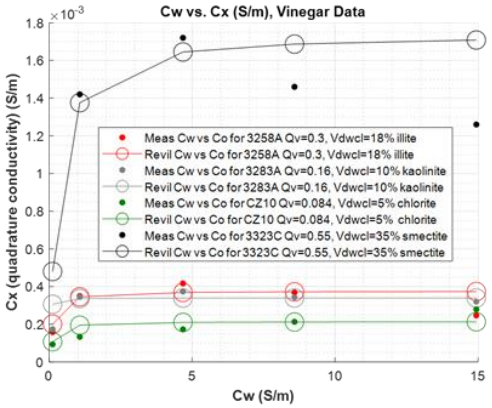

Fig. 15—Modeled and measured quadrature conductivity for four measured samples as a function of salinity.

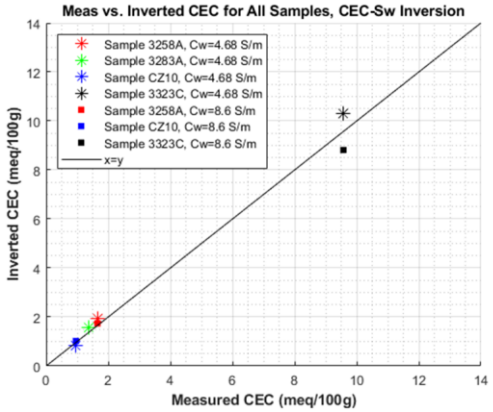

Fig. 16—Inverted and measured *CEC* for Cw=4.68 and 8.6 S/m for four samples having different clay volumes and types.

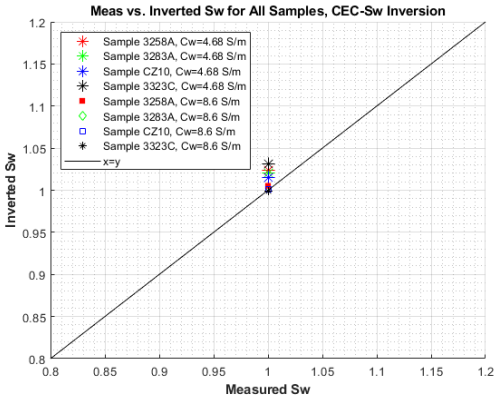

Fig. 17—Inverted and measured S_w for Cw=4.68 and 8.6 S/m for four samples having different clay volumes and types.

SUMMARY

We have reviewed the main fundamental flaws of the WS and DW petrophysical models. The primary flaw in the WS model is that it is not a truly parallel conductivity model. The DW model resolved this issue by treating the clay water and non-clay water as separate volumes with distinct conductivities. The DW model should be considered an improvement and upgrade from the WS model as it has remedied this primary flaw in the WS model.

However, the DW model is not easily implemented in practice as several computations such as NaCl activity and NaCl molarity are required but were not explicitly given in the published papers. We found that the model as put into practice limited the fractional volume of clay water to be less than or equal to the total fractional volume of water as it should be, however the published model did not. The model as put into practice has an inferior fit to the low salinity data compared to the published model. A secondary issue is that the more accurate algorithms to convert from salinity to conductivity as a function of temperature were not published and are not reflected in any published charts.

Neither WS nor DW models fit the very low salinity data very well. A dilution term for the counterion conductivity as a function of C_w was introduced in previous DW reference papers based on an incorrect unlimited diffuse layer expansion term but never put into practice. It was necessary to derive a new dilution factor based on the limited diffuse layer expansion. Writing this factor as a function of both clay type and salinity greatly improves the fit of the modeled to measured data at the very low salinities.

Both models suffer inaccuracies from the use of Q_{v_chem} instead of Q_{v_elec}. Both the WS B and DW β are derived from conductivity measurements that are influenced by all of the various ion species present in the clay water. Using a chemical derived CEC is incompatible with using a measured conductivity derived B or β. This issue is alleviated by using Q_{v_elec}.

We found from the measured conductivities taken at multiple salinities that Q_{v_elec} can be anywhere from equal to Q_{v_chem} to up to 50% higher than Q_{v_chem}. The lack of multiple-salinity conductivity measurements downhole requires a new technique to determine Q_{v_elec}. We illustrate how this is accomplished by incorporating the laboratory quadrature or out-of-phase measured conductivities with the measured in-phase conductivities. Work is in progress to apply this technique to downhole measured low frequency quadrature conductivities.

	WS Models				DW Models			
	A	B	C	D	E	F	G	H
	Waxman Smits original 1968 B, Qv_chem	Waxman Thomas 1974 B, Qv_chem	Juhasz 1981 B, Qv_chem	Waxman Thomas 1974 B, Qv_elect	DW as published, 1977, Qv_elec	DW with alpha limited, 1977 β, Qv_elec	DW with alpha limited, 2023 β diluted, Qv_elec	DW with alpha limited, 2023 β diluted, Qv_chem
Var $(S/m)^2$	64.4×10^{-5}	98.1×10^{-5}	118.0×10^{-5}	65.6×10^{-5}	8.66×10^{-5}	9.54×10^{-5}	2.78×10^{-5}	27.9×10^{-5}

Table 1—Computed "goodness-of-fit" for the various models for the 27 samples analyzed from WS Group 2 database. A total of 238 C_o, C_w data pairs are in the database. Columns A-D are the WS model with various relationships for B used and columns E-H are the Dual Water model with various techniques applied.

	Unlimited alpha, Swt=1, 71 deg F																								
Sample Number	**1**	**2**	**3**	**4**	**5**	**6**	**7**	**8**	**9**	**10**	**11**	**12**	**13**	**14**	**15**	**16**	**17**	**18**	**19**	**20**	**21**	**22**	**23**	**24**	**25**	**26**
Clay Fraction																										
% Kaolinite	100	90	90	100	100	90	100	100	90	65	65	100	100	100	100	100	100	20	20	20	12	12	8	12	0	0
% Illite	0	8	8	0	0	8	0	0	8	35	35	0	0	0	0	0	0	40	40	40	8	8	8	8	0	0
% Chlorite	0	3	3	0	0	3	0	0	3	0	0	0	0	0	0	0	0	0	0	0	0	0	0	0	0	0
% Smectite	0	0	0	0	0	0	0	0	0	0	0	0	0	0	0	0	0	20	20	20	80	80	84	80	100	100
Porosity	0.239	0.212	0.231	0.080	0.154	0.215	0.171	0.171	0.199	0.125	0.125	0.110	0.110	0.110	0.092	0.103	0.140	0.259	0.259	0.259	0.238	0.225	0.242	0.216	0.187	0.229
Qv_chemical	***0.02***	***0.05***	***0.05***	***0.26***	***0.20***	***0.10***	***0.05***	***0.05***	***0.09***	***0.09***	***0.09***	***0.28***	***0.28***	***0.28***	***0.41***	***0.67***	***0.33***	***0.59***	***0.59***	***0.59***	***0.29***	***0.72***	***1.04***	***0.81***	***1.27***	***1.47***
Qv_electrical	***0.13***	***0.13***	***0.15***	***0.12***	***0.18***	***0.18***	***0.31***	***0.31***	***0.19***	***0.03***	***0.39***	***0.51***	***0.65***	***0.61***	***0.92***	***0.95***	***0.94***	***0.85***	***0.73***	***0.59***	***0.32***	***1.17***	***1.34***	***1.45***	***1.68***	***1.74***
Cw 25.05	1.00	1.00	1.00	1.00	1.00	1.00	1.00	1.00	1.00	1.00	1.00	1.00	1.00	1.00	1.00	1.00	1.00	1.00	1.00	1.00	1.00	1.00	1.00	1.00	1.00	1.00
23.35	1.00	1.00	1.00	1.00	1.00	1.00	1.00	1.00	1.00	1.00	1.00	1.00	1.00	1.00	1.00	1.00	1.00	1.00	1.00	1.00	1.00	1.00	1.00	1.00	1.00	1.00
19.22	1.00	1.00	1.00	1.00	1.00	1.00	1.00	1.00	1.00	1.00	1.00	1.00	1.00	1.00	1.00	1.00	1.00	1.00	1.00	1.00	1.00	1.00	1.00	1.00	1.00	1.00
16.00	1.00	1.00	1.00	1.00	1.00	1.00	1.00	1.00	1.00	1.00	1.00	1.00	1.00	1.00	1.00	1.00	1.00	1.00	1.00	1.00	1.00	1.00	1.00	1.00	1.00	1.00
13.98	1.00	1.00	1.00	1.00	1.00	1.00	1.00	1.00	1.00	1.00	1.00	1.00	1.00	1.00	1.00	1.00	1.00	1.00	1.00	1.00	1.00	1.00	1.00	1.00	1.00	1.00
9.45	1.00	1.00	1.00	1.00	1.00	1.00	1.00	1.00	1.00	1.00	1.00	1.00	1.00	1.00	1.00	1.00	1.00	1.00	1.00	1.00	1.00	1.00	1.00	1.00	1.00	1.00
5.25	1.00	1.00	1.00	1.00	1.00	1.00	1.00	1.00	1.00	1.00	1.00	1.00	1.00	1.00	1.00	1.00	1.00	1.00	1.00	1.00	1.00	1.00	1.00	1.00	1.00	1.00
2.82	1.03	1.03	1.03	1.03	1.03	1.03	1.03	1.03	1.03	1.03	1.03	1.03	1.03	1.03	1.03	1.03	1.03	1.03	1.03	1.03	1.03	1.03	1.03	1.03	1.03	1.03
1.49	1.43	1.43	1.43	1.43	1.43	1.43	1.43	1.43	1.43	1.43	1.43	1.43	1.43	1.43	1.43	1.43	1.43	1.43	1.43	1.43	1.43	1.43	1.43	1.43	1.43	1.43
0.78	1.98	1.98	1.98	1.98	1.98	1.98	1.98	1.98	1.98	1.98	1.98	1.98	1.98	1.98	1.98	1.98	1.98	1.98	1.98	1.98	1.98	1.98	1.98	1.98	1.98	1.98
0.40	2.73	2.73	2.73	2.73	2.73	2.73	2.73	2.73	2.73	2.73	2.73	2.73	2.73	2.73	2.73	2.73	2.73	2.73	2.73	2.73	2.73	2.73	2.73	2.73	2.73	2.73
0.21	3.78	3.78	3.78	3.78	3.78	3.78	3.78	3.78	3.78	3.78	3.78	3.78	3.78	3.78	3.78	3.78	3.78	3.78	3.78	3.78	3.78	3.78	3.78	3.78	3.78	3.78
0.0001	38.01	38.01	38.01	38.01	38.01	38.01	38.01	38.01	38.01	38.01	38.01	38.01	38.01	38.01	38.01	38.01	38.01	38.01	38.01	38.01	38.01	38.01	38.01	38.01	38.01	38.01

Table 2—Computed and unlimited alpha for the 27 samples studied when the term $\alpha v_Q^H Q_v$ is allowed to exceed S_{wT} as originally presented in Clavier et. al. (1977, 1984). The case for $S_{wT} = 1$ and temperature of 71.6 °F is used. The value of alpha depends only on pore water salinity or C_w as expressed in Eq. (9). Alpha is unity at high salinities, then expands as salinity decreases.

	Limited alpha, Swt=1, 71 deg F																								
Sample Number	**1**	**2**	**3**	**4**	**5**	**6**	**7**	**8**	**9**	**10**	**11**	**12**	**13**	**14**	**15**	**16**	**17**	**18**	**19**	**20**	**21**	**22**	**23**	**24**	**25**	**26**
Qv_chemical	***0.02***	***0.05***	***0.05***	***0.26***	***0.20***	***0.10***	***0.05***	***0.05***	***0.09***	***0.09***	***0.09***	***0.28***	***0.28***	***0.28***	***0.41***	***0.67***	***0.33***	***0.59***	***0.59***	***0.59***	***0.29***	***0.72***	***1.04***	***0.81***	***1.27***	***1.47***
Qv_electrical	***0.13***	***0.13***	***0.15***	***0.12***	***0.18***	***0.18***	***0.31***	***0.31***	***0.19***	***0.03***	***0.39***	***0.51***	***0.65***	***0.61***	***0.92***	***0.95***	***0.94***	***0.85***	***0.73***	***0.59***	***0.32***	***1.17***	***1.34***	***1.45***	***1.68***	***1.74***
Cw 25.05	1.00	1.00	1.00	1.00	1.00	1.00	1.00	1.00	1.00	1.00	1.00	1.00	1.00	1.00	1.00	1.00	1.00	1.00	1.00	1.00	1.00	1.00	1.00	1.00	1.00	1.00
23.35	1.00	1.00	1.00	1.00	1.00	1.00	1.00	1.00	1.00	1.00	1.00	1.00	1.00	1.00	1.00	1.00	1.00	1.00	1.00	1.00	1.00	1.00	1.00	1.00	1.00	1.00
19.22	1.00	1.00	1.00	1.00	1.00	1.00	1.00	1.00	1.00	1.00	1.00	1.00	1.00	1.00	1.00	1.00	1.00	1.00	1.00	1.00	1.00	1.00	1.00	1.00	1.00	1.00
16.00	1.00	1.00	1.00	1.00	1.00	1.00	1.00	1.00	1.00	1.00	1.00	1.00	1.00	1.00	1.00	1.00	1.00	1.00	1.00	1.00	1.00	1.00	1.00	1.00	1.00	1.00
13.98	1.00	1.00	1.00	1.00	1.00	1.00	1.00	1.00	1.00	1.00	1.00	1.00	1.00	1.00	1.00	1.00	1.00	1.00	1.00	1.00	1.00	1.00	1.00	1.00	1.00	1.00
9.45	1.00	1.00	1.00	1.00	1.00	1.00	1.00	1.00	1.00	1.00	1.00	1.00	1.00	1.00	1.00	1.00	1.00	1.00	1.00	1.00	1.00	1.00	1.00	1.00	1.00	1.00
5.25	1.00	1.00	1.00	1.00	1.00	1.00	1.00	1.00	1.00	1.00	1.00	1.00	1.00	1.00	1.00	1.00	1.00	1.00	1.00	1.00	1.00	1.00	1.00	1.00	1.00	1.00
2.82	1.03	1.03	1.03	1.03	1.03	1.03	1.03	1.03	1.03	1.03	1.03	1.03	1.03	1.03	1.03	1.03	1.03	1.03	1.03	1.03	1.03	1.03	1.03	1.03	1.03	1.03
1.49	1.43	1.43	1.43	1.43	1.43	1.43	1.43	1.43	1.43	1.43	1.43	1.43	1.43	1.43	1.43	1.43	1.43	1.43	1.43	1.43	1.43	1.43	1.43	1.43	1.43	1.43
0.78	1.98	1.98	1.98	1.98	1.98	1.98	1.98	1.98	1.98	1.98	1.98	1.98	1.98	1.98	1.98	1.98	1.98	1.98	1.98	1.98	1.98	1.98	1.98	1.98	1.94	1.88
0.40	2.73	2.73	2.73	2.73	2.73	2.73	2.73	2.73	2.73	2.73	2.73	2.73	2.73	2.73	2.73	2.73	2.73	2.73	2.73	2.73	2.73	2.73	2.45	2.27	1.94	1.88
0.21	3.78	3.78	3.78	3.78	3.78	3.78	3.78	3.78	3.78	3.78	3.78	3.78	3.78	3.78	3.56	3.46	3.49	3.78	3.78	3.78	3.78	2.79	2.45	2.27	1.94	1.88
0.0001	25.43	25.09	21.88	26.97	18.04	17.76	10.51	10.45	17.28	38.01	8.46	6.40	5.02	5.35	3.56	3.46	3.49	3.85	4.46	5.58	10.23	2.79	2.45	2.27	1.94	1.88

Table 3—Computed limited alpha for the 27 samples studied when the term $\alpha v_Q^H Q_v$ is ***not*** allowed to exceed S_{wT} (see Eq. 29) The case for $S_{wT} = 1$ and temperature of 71.6 °F is used. Because the term $\alpha v_Q^H Q_v$ will exceed $S_{wT} = 1$ sooner for higher values of Q_v , at any given pore water salinity or C_w, the limited alpha will depend on both salinity and Q_v. When the clay water fills the pore space, we limit alpha. The shading shows where alpha has been limited.

	αVqhQv limited to 1, Swt=1.0, 71 deg F																								
Sample Number	**1**	**2**	**3**	**4**	**5**	**6**	**7**	**8**	**9**	**10**	**11**	**12**	**13**	**14**	**15**	**16**	**17**	**18**	**19**	**20**	**21**	**22**	**23**	**24**	**25**	**26**
Qv_chemical	***0.02***	***0.05***	***0.05***	***0.26***	***0.20***	***0.10***	***0.05***	***0.05***	***0.09***	***0.09***	***0.09***	***0.28***	***0.28***	***0.28***	***0.41***	***0.67***	***0.33***	***0.59***	***0.59***	***0.59***	***0.29***	***0.72***	***1.04***	***0.81***	***1.27***	***1.47***
Qv_electrical	***0.13***	***0.13***	***0.15***	***0.12***	***0.18***	***0.18***	***0.31***	***0.31***	***0.19***	***0.03***	***0.39***	***0.51***	***0.65***	***0.61***	***0.92***	***0.95***	***0.94***	***0.85***	***0.73***	***0.59***	***0.32***	***1.17***	***1.34***	***1.45***	***1.68***	***1.74***
Cw 25.05	0.04	0.04	0.05	0.04	0.06	0.06	0.10	0.10	0.06	0.01	0.12	0.16	0.20	0.19	0.28	0.29	0.29	0.26	0.22	0.18	0.10	0.36	0.41	0.44	0.51	0.53
23.35	0.04	0.04	0.05	0.04	0.06	0.06	0.10	0.10	0.06	0.01	0.12	0.16	0.20	0.19	0.28	0.29	0.29	0.26	0.22	0.18	0.10	0.36	0.41	0.44	0.51	0.53
19.22	0.04	0.04	0.05	0.04	0.06	0.06	0.10	0.10	0.06	0.01	0.12	0.16	0.20	0.19	0.28	0.29	0.29	0.26	0.22	0.18	0.10	0.36	0.41	0.44	0.51	0.53
16.00	0.04	0.04	0.05	0.04	0.06	0.06	0.10	0.10	0.06	0.01	0.12	0.16	0.20	0.19	0.28	0.29	0.29	0.26	0.22	0.18	0.10	0.36	0.41	0.44	0.51	0.53
13.98	0.04	0.04	0.05	0.04	0.06	0.06	0.10	0.10	0.06	0.01	0.12	0.16	0.20	0.19	0.28	0.29	0.29	0.26	0.22	0.18	0.10	0.36	0.41	0.44	0.51	0.53
9.45	0.04	0.04	0.05	0.04	0.06	0.06	0.10	0.10	0.06	0.01	0.12	0.16	0.20	0.19	0.28	0.29	0.29	0.26	0.22	0.18	0.10	0.36	0.41	0.44	0.51	0.53
5.25	0.04	0.04	0.05	0.04	0.06	0.06	0.10	0.10	0.06	0.01	0.12	0.16	0.20	0.19	0.28	0.29	0.29	0.26	0.22	0.18	0.10	0.36	0.41	0.44	0.51	0.53
2.82	0.04	0.04	0.05	0.04	0.06	0.06	0.10	0.10	0.06	0.01	0.12	0.16	0.21	0.19	0.29	0.30	0.30	0.27	0.23	0.19	0.10	0.37	0.42	0.46	0.53	0.55
1.49	0.06	0.06	0.07	0.05	0.08	0.08	0.14	0.14	0.08	0.01	0.17	0.22	0.29	0.27	0.40	0.41	0.41	0.37	0.32	0.26	0.14	0.51	0.59	0.63	0.74	0.76
0.78	0.08	0.08	0.09	0.07	0.11	0.11	0.19	0.19	0.11	0.02	0.23	0.31	0.39	0.37	0.56	0.57	0.57	0.51	0.44	0.35	0.19	0.71	0.81	0.87	1.00	1.00
0.40	0.11	0.11	0.12	0.10	0.15	0.15	0.26	0.26	0.16	0.02	0.32	0.43	0.54	0.51	0.77	0.79	0.78	0.71	0.61	0.49	0.27	0.98	1.00	1.00	1.00	1.00
0.21	0.15	0.15	0.17	0.14	0.21	0.21	0.36	0.36	0.22	0.03	0.45	0.59	0.75	0.71	1.00	1.00	1.00	0.98	0.85	0.68	0.37	1.00	1.00	1.00	1.00	1.00
0.0001	1.00	1.00	1.00	1.00	1.00	1.00	1.00	1.00	1.00	0.32	1.00	1.00	1.00	1.00	1.00	1.00	1.00	1.00	1.00	1.00	1.00	1.00	1.00	1.00	1.00	1.00

Table 4— Computed limited $\alpha v_Q^H Q_v$ for the 27 samples studied when the term $\alpha v_Q^H Q_v$ is ***not*** allowed to exceed S_{wT}. The case for $S_{wT} = 1.0$ and temperature of 71.6 °F is used.

	αVqhQv limited to 0.50, Swt=0.50, 150 deg F																								
Sample Number	1	2	3	4	5	6	7	8	9	10	11	12	13	14	15	16	17	18	19	20	21	22	23	24	25	26
Qv_chemical	*0.02*	*0.05*	*0.05*	*0.26*	*0.20*	*0.10*	*0.05*	*0.05*	*0.09*	*0.09*	*0.09*	*0.28*	*0.28*	*0.28*	*0.41*	*0.67*	*0.33*	*0.59*	*0.59*	*0.59*	*0.29*	*0.72*	*1.04*	*0.81*	*1.27*	*1.47*
Qv_electrical	*0.13*	*0.13*	*0.15*	*0.12*	*0.18*	*0.18*	*0.31*	*0.31*	*0.19*	*0.03*	*0.39*	*0.51*	*0.65*	*0.61*	*0.92*	*0.95*	*0.94*	*0.85*	*0.73*	*0.59*	*0.32*	*1.17*	*1.34*	*1.45*	*1.68*	*1.74*
Cw 25.05	0.03	0.03	0.04	0.03	0.05	0.05	0.08	0.08	0.05	0.01	0.10	0.14	0.17	0.16	0.24	0.25	0.25	0.23	0.20	0.16	0.09	0.31	0.36	0.38	0.45	0.46
23.35	0.03	0.03	0.04	0.03	0.05	0.05	0.08	0.08	0.05	0.01	0.10	0.14	0.17	0.16	0.24	0.25	0.25	0.23	0.20	0.16	0.09	0.31	0.36	0.38	0.45	0.46
19.22	0.03	0.03	0.04	0.03	0.05	0.05	0.08	0.08	0.05	0.01	0.10	0.14	0.17	0.16	0.24	0.25	0.25	0.23	0.20	0.16	0.09	0.31	0.36	0.38	0.45	0.46
16.00	0.03	0.03	0.04	0.03	0.05	0.05	0.08	0.08	0.05	0.01	0.10	0.14	0.17	0.16	0.24	0.25	0.25	0.23	0.20	0.16	0.09	0.31	0.36	0.38	0.45	0.46
13.98	0.03	0.03	0.04	0.03	0.05	0.05	0.08	0.08	0.05	0.01	0.10	0.14	0.17	0.16	0.24	0.25	0.25	0.23	0.20	0.16	0.09	0.31	0.36	0.38	0.45	0.46
9.45	0.03	0.03	0.04	0.03	0.05	0.05	0.08	0.08	0.05	0.01	0.10	0.14	0.17	0.16	0.24	0.25	0.25	0.23	0.20	0.16	0.09	0.31	0.36	0.38	0.45	0.46
5.25	0.04	0.04	0.04	0.04	0.05	0.05	0.09	0.09	0.06	0.01	0.11	0.15	0.19	0.18	0.27	0.28	0.28	0.25	0.22	0.17	0.09	0.35	0.40	0.43	0.50	0.50
2.82	0.05	0.05	0.06	0.05	0.07	0.07	0.13	0.13	0.08	0.01	0.16	0.21	0.26	0.25	0.37	0.38	0.38	0.34	0.30	0.24	0.13	0.48	0.50	0.50	0.50	0.50
1.49	0.07	0.07	0.08	0.07	0.10	0.10	0.17	0.17	0.11	0.02	0.21	0.28	0.36	0.34	0.50	0.50	0.50	0.47	0.41	0.33	0.18	0.50	0.50	0.50	0.50	0.50
0.78	0.10	0.10	0.11	0.09	0.14	0.14	0.24	0.24	0.14	0.02	0.29	0.39	0.50	0.47	0.50	0.50	0.50	0.50	0.50	0.45	0.24	0.50	0.50	0.50	0.50	0.50
0.40	0.14	0.14	0.16	0.13	0.19	0.19	0.33	0.33	0.20	0.03	0.41	0.50	0.50	0.50	0.50	0.50	0.50	0.50	0.50	0.50	0.34	0.50	0.50	0.50	0.50	0.50
0.21	0.19	0.19	0.22	0.18	0.26	0.27	0.45	0.45	0.27	0.04	0.50	0.50	0.50	0.50	0.50	0.50	0.50	0.50	0.50	0.50	0.46	0.50	0.50	0.50	0.50	0.50
0.0001	0.50	0.50	0.50	0.50	0.50	0.50	0.50	0.50	0.50	0.27	0.50	0.50	0.50	0.50	0.50	0.50	0.50	0.50	0.50	0.50	0.50	0.50	0.50	0.50	0.50	0.50

Table 5— Computed limited $\alpha v_Q^H Q_v$ for the 27 samples studied when the term $\alpha v_Q^H Q_v$ is ***not*** allowed to exceed S_{wT}. The case for hydrocarbon bearing, downhole conditions of $S_{wT} = 0.50$ and temperature of 150 °F is used. The quantity $\alpha v_Q^H Q_v$ becomes limited at higher salinities for more of the samples.

	αVqhQv limited to 0.25, Swt=0.25, 150 deg F																								
Sample Number	1	2	3	4	5	6	7	8	9	10	11	12	13	14	15	16	17	18	19	20	21	22	23	24	25	26
Qv_chemical	*0.02*	*0.05*	*0.05*	*0.26*	*0.20*	*0.10*	*0.05*	*0.05*	*0.09*	*0.09*	*0.09*	*0.28*	*0.28*	*0.28*	*0.41*	*0.67*	*0.33*	*0.59*	*0.59*	*0.59*	*0.29*	*0.72*	*1.04*	*0.81*	*1.27*	*1.47*
Qv_electrical	*0.13*	*0.13*	*0.15*	*0.12*	*0.18*	*0.18*	*0.31*	*0.31*	*0.19*	*0.03*	*0.39*	*0.51*	*0.65*	*0.61*	*0.92*	*0.95*	*0.94*	*0.85*	*0.73*	*0.59*	*0.32*	*1.17*	*1.34*	*1.45*	*1.68*	*1.74*
Cw 25.05	0.03	0.03	0.04	0.03	0.05	0.05	0.08	0.08	0.05	0.01	0.10	0.14	0.17	0.16	0.24	0.25	0.25	0.23	0.20	0.16	0.09	0.25	0.25	0.25	0.25	0.25
23.35	0.03	0.03	0.04	0.03	0.05	0.05	0.08	0.08	0.05	0.01	0.10	0.14	0.17	0.16	0.24	0.25	0.25	0.23	0.20	0.16	0.09	0.25	0.25	0.25	0.25	0.25
19.22	0.03	0.03	0.04	0.03	0.05	0.05	0.08	0.08	0.05	0.01	0.10	0.14	0.17	0.16	0.24	0.25	0.25	0.23	0.20	0.16	0.09	0.25	0.25	0.25	0.25	0.25
16.00	0.03	0.03	0.04	0.03	0.05	0.05	0.08	0.08	0.05	0.01	0.10	0.14	0.17	0.16	0.24	0.25	0.25	0.23	0.20	0.16	0.09	0.25	0.25	0.25	0.25	0.25
13.98	0.03	0.03	0.04	0.03	0.05	0.05	0.08	0.08	0.05	0.01	0.10	0.14	0.17	0.16	0.24	0.25	0.25	0.23	0.20	0.16	0.09	0.25	0.25	0.25	0.25	0.25
9.45	0.03	0.03	0.04	0.03	0.05	0.05	0.08	0.08	0.05	0.01	0.10	0.14	0.17	0.16	0.24	0.25	0.25	0.23	0.20	0.16	0.09	0.25	0.25	0.25	0.25	0.25
5.25	0.04	0.04	0.04	0.04	0.05	0.05	0.09	0.09	0.06	0.01	0.11	0.15	0.19	0.18	0.25	0.25	0.25	0.25	0.22	0.17	0.09	0.25	0.25	0.25	0.25	0.25
2.82	0.05	0.05	0.06	0.05	0.07	0.07	0.13	0.13	0.08	0.01	0.16	0.21	0.25	0.25	0.25	0.25	0.25	0.25	0.25	0.24	0.13	0.25	0.25	0.25	0.25	0.25
1.49	0.07	0.07	0.08	0.07	0.10	0.10	0.17	0.17	0.11	0.02	0.21	0.25	0.25	0.25	0.25	0.25	0.25	0.25	0.25	0.25	0.18	0.25	0.25	0.25	0.25	0.25
0.78	0.10	0.10	0.11	0.09	0.14	0.14	0.24	0.24	0.14	0.02	0.25	0.25	0.25	0.25	0.25	0.25	0.25	0.25	0.25	0.25	0.24	0.25	0.25	0.25	0.25	0.25
0.40	0.14	0.14	0.16	0.13	0.19	0.19	0.25	0.25	0.20	0.03	0.25	0.25	0.25	0.25	0.25	0.25	0.25	0.25	0.25	0.25	0.25	0.25	0.25	0.25	0.25	0.25
0.21	0.19	0.19	0.22	0.18	0.25	0.25	0.25	0.25	0.25	0.04	0.25	0.25	0.25	0.25	0.25	0.25	0.25	0.25	0.25	0.25	0.25	0.25	0.25	0.25	0.25	0.25
0.0001	0.25	0.25	0.25	0.25	0.25	0.25	0.25	0.25	0.25	0.25	0.25	0.25	0.25	0.25	0.25	0.25	0.25	0.25	0.25	0.25	0.25	0.25	0.25	0.25	0.25	0.25

Table 6— Computed limited $\alpha v_Q^H Q_v$ for the 27 samples studied when the term $\alpha v_Q^H Q_v$ is ***not*** allowed to exceed S_{wT}. The case for hydrocarbon bearing, downhole conditions of $S_{wT} = 0.25$ and temperature of 150 °F is used. The quantity $\alpha v_Q^H Q_v$ becomes limited at higher salinities for more of the samples compared to table 5.

NOMENCLATURE

Abbreviations

IET Institute of Engineering and Technology

CEC cation exchange capacity (dry rock), meq/100 g.

SEM scanning electron microscope

OHP Outer Helmholtz plane

Notations and Units

A_{sp} specific area of clay surface, m^2/g.

A_v clay surface area per unit of PV, m^2/cm^3.

B equivalent conductivity of clay cations, WS model (S/m) / (meq/cm^3) [(S/m)/(meq/mL)]. Dimensional analysis reveals it to be an "equivalent molar conductivity."

B_i $1/F_0$

B_0 constant value of B at high water salinities, $B_0 = C_x lQ_v$, (S/m)/(meq/cm^3) [(S/m)/(meq/mL)]

C_{cw} conductivity of clay-water, S/m.

C_w conductivity of formation brine S/m.

C_{we} effective conductivity of water in a shaly sand S/m.

C_x intercept of linear portion of C_0 vs. C_w curve extrapolated to C_w axis ($C_x = BQ_v$) S/m.

C_t true conductivity of (hydrocarbon- bearing) formation, S/m.

C_0 conductivity of 100% water-saturated formation

C_{0c} computed formation conductivities, S/m.

C_{0m} measured formation conductivities, S/m [mho/m]

C_ℓ the C_w value above which C_0 varies linearly with C_w, S/m.

F formation resistivity factor for a clean sand, $F = R_0/R_w$.

F_0 formation resistivity factor for a shaly sand as used in DW shaly sand model.

F^* formation resistivity factor for a shaly sand as used in WS shaly sand model. $F^* = R_0/R_{we}$.

$\mathcal{F}$ Faraday's constant 96,485 coulombs/equivalent.

N_A Avogadro's number 6.022×10^{23} particles/mole

$Q_{v\_chemical}$ concentration of clay counterions per unit PV, meq/cm^3 determined from chemical methods.

$Q_{velectrical}$ Q_v computed from intercept C_x of C_0-C_w plot.

R_0 resistivity of brine-saturated formation, Ω-m.

R_t "true" formation resistivity, Ω-m.

R_w formation brine resistivity, Ω-m.

S_{wT} fraction of total porosity filled with connate and clay water

S_w^n S_w (or S_{wT}) to n^{th} power

$T_{\text{°C}}$ temperature in °C.

$T_{\text{°K}}$ temperature in °K.

T_0 reference temperature, °K.

V_{cw} fractional volume of "clay" water

V_{fw} fractional volume of "far" water

Y amount of clay normalized to fraction of solids volume. $Y = Q_v\, \varphi_t / (1 - \varphi_t)$

m porosity exponent

n saturation exponent

$\langle n \rangle$ salt concentration in brine, mol/dm^3 [mol/L]

$\langle n_\ell \rangle$ lower limit of linear segment of C_0-C_w plot. $\langle n_\ell \rangle > 1 \Rightarrow \alpha = 1$.

n_i $\left[\dfrac{\text{particles}}{\text{unit volume}}\right] \equiv \left[\dfrac{\text{ions}}{\text{cm}^3}\right]$

q_i total charge on an ion (coulombs/ion)

r_{Na} radius of sodium ion, Å = 10^{-10} m.

r_w "radius" of water molecule, Å = 10^{-10} m.

s slope of C_0 vs. C_w curve for $C_w > C_\ell$.

v_Q $v x_H = A_v\, x_H / Q_v$, cm^3/meq..

v_Q^H volume of clay water per counter ion at 22° C and when $\alpha = 1$.

$v_Q^H(T)$ v_Q^H at temperature T°K.

x_d thickness of diffuse layer, in Å = 10^{-10} m.

x_H distance to OHP from clay surface, 6.18 Å.

Λ molar conductivity of electrolyte

α diffuse layer expansion factor.

β Clavier et al. define as "equivalent conductivity" to align with WS use of this definition for B. The molar conductivity of sodium counterions;

β_{dil} diffuse layer expansion factor.

$\beta_{T_{\text{°C}}}$ β values at temperature T.

γ NaCl activity coefficient.

λ molar conductivity of ion species; Waxman and Smits call this parameter "equivalent conductivity", which term is also adopted and Clavier et al.

v specific clay area coefficient, m^2/cm^3.

μ_i mobility of i^{th} species of ion; [speed/potential gradient]

φ_t total porosity as fractional volume of rock (v/v)

REFERENCES

Clavier, C., Coates, G., Dumanoir, J., 1977, The Theoretical and Experimental Basis for the Dual Water Model for the Interpretation of Shaly Sands, presented at 52nd Annual Fall Technical Conference in Denver, CO., SPE 6859. SPE J. Vol. 24, Issue 02 p. 153–168. SPE-6859-PA https://doi.org/10.2118/6859-PA

Clavier, C., Coates, G., Dumanoir, J., 1984, Theoretical and Experimental Basis for the Dual Water Model for Interpretation for Shaly Sands, SPE Journal April 1984.

Juhasz, I., 1979, The Central Role of Q_v and Evaluation of Shaly Formations, *The Log Analyst*, July-August, p. 3-13.

Juhasz, I., 1981, Normalized Q_v – The Key to Shaly Sand Evaluation Using the Waxman-Smits Equation in the Absence of Core Data, *Transactions*, SPWLA 22nd Annual Logging Symposium, June 23-26, Z.

Maxwell, J. C., 1873, *A Treatise on Electromagnetism*, 1873, Cambridge University Press, Chapter VI, Paragraph 277, p 331, Formula (7).

National Research Council, 1933, *International Critical Tables of Numerical Data, Chemistry and Technology*, McGraw-Hill, New York.

Revil, A., 2012, Spectral Induced Polarization of Shaly Sands Influence of the Electrical Double Layer, Water Resources Research, Vol 48, Issue 2, Feb., W02517,- https://doi.org/10.1029/2011WR011260.

Simandoux, P., 1963, (Translated by L. Moinard, in the SPWLA Shaly Sand Reprint Volume)- 1982, Dielectric Measurements On Porous Media, Application To The Measurement of Water Saturations, Study of The Behavior of Argillaceous Formations, *Revue de l'Institut Francais du Petrole*, p. 193-215.

Truesdell, A. H., 1968, Activity Coefficients of Aqueous Sodium Chloride from 15 to 50 °C Measured with a Glass Electrode. *Science*, Vol. 161 No. 3844, p. 884–886 https://doi.org/10.1126/science.161.3844.884

Van Olphen, H., Waxman, M. H., 1958, Surface Conductance of Sodium Bentonite in Water, Clays and Clay Minerals, Proc., 5th Natl. Conference of Clays and Minerals, Natl. Academy of Science/Natl. Research Council, Washington, D.C.

Vinegar, H.J., Waxman, M. H, 1984, Induced Polarization of Shaly Sands, Geophysics, Vol. 49, Issue 8, p. 1267–1287 https://doi.org/10.1190/1.1441755

Waxman, M., H., Smits, L., J., M., 1968, Electrical Conductivities in Oil-Bearing Shaly Sands, SPE Annual Fall Meeting, Houston TX., Oct 1-4, 1967, SPE Transactions Volume 243, 1968.

Waxman, M., H., Thomas E. C., 1974, Electrical Conductivities in Shaly sands – I. The Relation Between Hydrocarbon Saturation and Resistivity Index; II. The Temperature Coefficient of Electrical Conductivity, Journal of Petroleum Technology, Feb 1974, 213-225.

Waxman, M., H., Thomas E. C., 2007, - Technical Note – An Addendum to Electrical Conductivities in Shaly Sands – I. The Relation Between Hydrocarbon Saturation and Resistivity Index; II. The Temperature Coefficient of Electrical Conductivity, *SPE J*, Vol. 12, Issue 4, p. 392 SPE-109632-PA https://doi.org/10.2118/109632-PA

ABOUT THE AUTHORS

John C. Rasmus retired from SLB in 2018. While at SLB he serves as an Advisor-Reservoir Characterization in the SLB LWD product line based in Sugar Land, TX. Duties included LWD interpretation field and client support, resistivity and nuclear interpretation support and special projects. Previously he held various interpretation positions developing new and innovative interpretation techniques for secondary porosity in carbonates, geo-steering of horizontal wells, geo-pressure quantification in under-compacted shales, downhole motor optimization and HAHZ well petrophysics. John holds a BS in mechanical engineering from Iowa State University in Ames Iowa and an MS in petroleum engineering from the University of Houston. John is a member of SPWLA, SPE, AAPG and is a registered professional petroleum engineer in Texas. John recently started Interfacial Polarization Dielectric Petrophysics LLC to develop and market interpretation methodologies for low frequency dielectric measurements. John can be contacted at 281-678-9325 or at **jrrasmus.tfs@gmail.com**

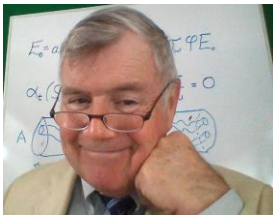

David Kennedy began a career in the logging industry in 1973 after earning a BS in Physics at Georgia Tech. He entered the industry as a Schlumberger field engineer in California and Alaska, staying with Schlumberger for five years. Following that, Dave returned to school and earned MS degrees in Physics and Earth Sciences at the University of Texas at Dallas, with further studies at U. C. Berkeley. In his career he has worked in one or another capacity at Arco, Sohio Research and Operations, Mobil Research and Operations, ExxonMobil Research and Operations, Baker-Hughes, PathFinder, Southwestern Energy and Texas A&M University. He did stay with Mobil and ExxonMobil for 20 years to prove to his mother he could hold a job! David has been an SPWLA member for 40 years and served as V.P. Publications and Editor of *Petrophysics* from 1999-2002, V.P. Technology in 2009, and President (etc.) from 2014-2016. David is an inventor or coinventor on six U.S. Patents, and has published about 60 articles as author or coauthor in conference proceedings and refereed journals. His major research interest has been formation conductivity interpretation and electromagnetic logging instrumentation. David has been an educator all his life, having taught courses at the USMA at West Point, courses in computer science, physics, materials science, and electrical engineering at San Francisco Bay Area private and junior colleges. He is now recently retired as a professor in the Petroleum Engineering Department at Texas A&M University where he instructed graduates and undergraduates in formation evaluation. Before all of that, David served as a Lieutenant of Infantry in Vietnam where he received both a Purple Heart and Bronze Star with V device.

david_kennedy@qed-petrophysics.com.

Dean M. Homan is an Advisor Research Scientist at SLB Houston Formation Evaluation Center, and has worked on triaxial antenna development, induction array design, tool calibration and resistivity environmental corrections since 1999. Dean is an author of 37 papers and holder of 45 patents. He was awarded the SPWLA Distinguished Technical Achievement Award in 2013 for significant contributions in electromagnetic logging. He was cited SPWLA Best Paper/Presentation in 2016 for his contribution to the electromagnetic look-ahead (EMLA) tool development. Before joining SLB, he held a post-doctoral position at Rice University, developing the degenerate Fermi gas experiment. He has a BS in physics and mathematics from University of Nebraska, Lincoln and a PhD in atomic experimental/theoretical physics from the University of Kentucky.

Dhoman@slb.com

APPENDIX A

REVIEW OF WAXMAN'S AND SMITS' MODEL

What the Paper Claims. Waxman's and Smits' 1968 "seminal" paper is confusing in several ways. Firstly, it self-proclaims two times that the model it describes is first "the model consists of two resistance elements in parallel" and secondly "conductivity equations based on a parallel conductivity model". Elsewhere in the text the paper asserts "We assume next that the electric current transported by the counterions associated with the clay travels along the same tortuous path as the current attributed to the ions in the pore water." These assertions are supported by the first two equations in the paper,

$$C_{rock} = C_c + C_{el} \tag{A.1}$$

and

$$C_0 = xC_e + yC_w \tag{A.2}$$

where the first equation is for the sum of conductances, *C*, and the second equation is for a weighted sum of conductivities, but denoted by the same notation, *C*. This clash of notations at the very beginning of the paper signals that the authors are a bit innocent of the relationship between conductance and conductivity and what is understood by the majority of the people who use the phrase when they hear "parallel conductivity" (see Fig. A.1). The assumption regarding the "same tortuous path" is also enigmatic for people familiar with clay-bearing pore spaces (see Fig. A.2).

*History***.** Rock conductivity is customarily characterized in terms of resistivity. The reasons for this are historical. Surface electrical prospecting methods recorded and displayed their results in terms of apparent resistivities. Well logging, descended from surface electrical prospecting techniques, continued the custom of presenting

results in terms of apparent resistivities. Accordingly, when measurement of the electrical properties of core plugs was developed, its results were also reported in terms of resistivity. Thus, the data available to the pioneer, G. E. Archie, was recorded as resistivity in both well logs and core reports. It would have been surprising if Archie had not used resistivity in the development of his pioneering model. We are still using Archie's model and apparent resistivities from logs to this day. In the present context, the Waxman-Smits model is designed to reduce to the Archie model (in its conductivity representation) in the limit of 0 counterion concentration, $Q_v = 0$.

Unfortunately, it is unlikely that any great intuition for conductivity in rocks can be developed by studying the resistivity representation of the Archie model. M. R. J. Wyllie writes in his 1963 book, *The Fundamentals of Well Log Interpretation*,

> In many ways it is unfortunate that conductivity was not selected in place of resistivity as the standard term in the early days of electrical logging. Conductivity logs, although identical in general form to resistivity logs, would somewhat simplify the equations now used in log interpretation. It is probably too late to upset the entire terminology of logging, but it is still sometimes easier to speak and think in terms of conductivities instead of resistivities.

Some theoretical models were, in fact, developed in conductivity terms, but still clinging to resistivity as the parameter. Wyllie (as coauthor with H. W. Patnode, 1949) himself introduced conductivity as reciprocal resistivity

$$\frac{1}{\rho_{wa}} = \frac{1}{\rho_f} + \frac{1}{\rho_w} = \frac{1}{\rho_f} + \frac{1}{F\rho_c} \qquad \text{(A.3)}$$

where all of the ρ variables are resistivities. As another example, Poupon et al. (1954) described the influence of shale upon bulk resistivity using the equation

$$\frac{1}{R_t} = \frac{V_{sh}}{R_{sh}} + \frac{1-V_{sh}}{R_t^*} \quad . \qquad \text{(A.4)}$$

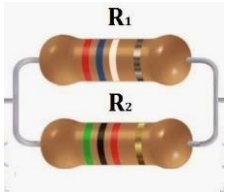

Fig. A1. An internet search for images of parallel resistor circuits results in numerous versions of the resistor pair shown here. Most readers will have been introduced to this concept of parallel resistors in high school and/or university physics.

This is clearly a volume weighted average of conductivities. There are many such examples in the literature of the late 1940s and 1950s but authors were not so bold as to switch explicitly to conductivity notation.

So indeed, while it seems to have been "too late" for practicing formation evaluators (and service companies, although early induction logs were presented in terms of conductivity) to make the paradigm shift to conductivity, theoretical petrophysicists (if anyone can be called by that name) did in fact begin to shift to a conductivity representation. For example, Simandoux's (1963) study is in conductivity terms. Waxman and Smits were among the first, if not the very first, writing in the English language literature to shift to a conductivity model for theoretical development.

The purpose of this appendix is to clarify the message of Waxman and Smits as presented in their 1968 seminal, but poorly understood, paper. The model had been in use by Shell petrophysicists for 14 years when, in 1981, Juhasz succeeded in explaining the W-S model to the larger world in simple straightforward terms

> … , the W-S conductivity model states that the conductivity behavior of a shaly sand is exactly the same as that of a hypothetical clean sand . . . having the same porosity and pore-geometrical parameters (m^*, n^*) as that of the shaly formation, except that the conductivity of the bulk water contained in it appears to be greater than the salinity of the equilibrating water (free electrolyte, or far-water in dual-water-model terminology) would indicate. The excess bulk water conductivity is due to the presence of excess cations in the bulk water surrounding the clay particles and compensating for their negative electrical charges. The magnitude of the excess conductivity is proportional to the concentration of

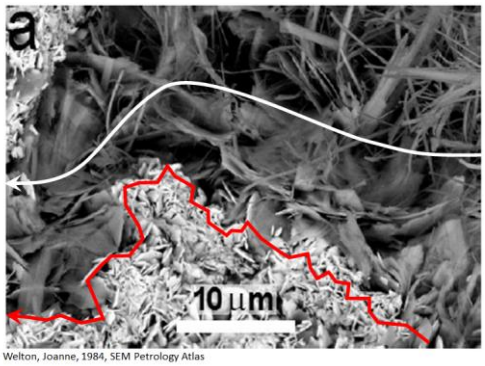

Fig. A2. Photomicrograph of clay-lined pore and the difference in the tortuous paths followed by "counterions associated with the clay"(red path) and "ions in the pore water" (white path).

these compensating cations (Q_v/S_{wT}) and their equivalent conductance, *B*. …

Stated even more briefly, the Waxman-Smits model is *formally* the *same* as the Archie model, but with a correction to the formation brine resistivity to account for the conductivity of cations associated with clays bounding some of the pore space.

Had the W-S introductory paper contained a similar summary as a preamble to the theoretical development, the paper might have been much better understood. Practical formation evaluators are most often probably trained in the application of the W-S model using the model as explained by Juhasz in several papers that appeared more than a decade following the original paper, and five years following its extension to hydrocarbon saturated reservoirs. People who prefer to start with original sources and work through a paper line-by-line are at a disadvantage because, to say the least, the development of the model in the paper is opaque and, seemingly, inconsistent until these readers can put their minds into the same headspace as Waxman and Smits. One of your authors (Kennedy) is an "original source" person; he could never read past equation (4) in the 1968 paper and did not become aware of Juhasz's contributions for a decade afterward. This appendix is for people who wish to understand the derivation in the original paper. We think of the process as "decoding".

Waxman and Smits (W-S) offer a derivation of their model using the sequence of five equations

$$C_{rock} = C_c + C_{el} \quad \ldots\ldots \quad (1)$$

$$C_o = xC_e + yC_w \quad \ldots\ldots \quad (2)$$

$$x = y = \frac{1}{F^*} \quad \ldots\ldots \quad (3)$$

$$C_o = \frac{1}{F^*}(C_e + C_w) \quad \ldots\ldots \quad (4)$$

$$C_e = \frac{\mathcal{F}\mu^e_{Na}}{1000} Q_v = \frac{\lambda^e_{Na}}{1000} Q_v \quad \ldots \quad (5)$$

The quantities denoted as "**C",** W-S equation (1), are *conductances*[1]. Using (SI) ***Système International*** and the (IET) Institution of Engineering and Technology recommended notation for these quantities, the equation would be written as

$$g_{rock} = g_c + g_{el}\,. \qquad \text{W-S (1)} \qquad (A.5)$$

g_{rock} denotes the equivalent conductance of a rock comprising two conductors[2] with conductances g_c and g_{el}. The subscript *c* denotes the "conductance contribution of cations associated with *c*lay" while *el* denotes the conductance contribution of the "free *el*ectrolyte contained in the pore volume of the rock". The formula applies to the two conductances on the right side of W-S (1) connected in "parallel". Indeed, Waxman and Smits introduce their model as "two resistance elements in parallel" and later refer to it as "a parallel conductance model".

Conductance is defined, using measurements, as the ratio of the current induced to flow through a conductor to the potential difference inducing the current, written as $g = I/V$. Alternatively, it is defined in terms of material properties as being proportional to the conductivity of the material comprising the conductor σ, proportional to its cross-sectional area *A*, and inversely proportional to its length *L*, or $g = (A/L)\sigma$, thus providing a means to determine a material's conductivity using a sample of uniform cross-sectional area *A* and length *L* by $\sigma = (L/A)(I/V)$.

The quantities denoted as "**C",** W-S equation (2), are *conductivities*; denoted by σ in SI notation. Translated into SI notational conventions, W-S (2) would be

$$\sigma_0 = x\sigma_e + y\sigma_w \qquad (A.6)$$

where the subscript *e* denotes the conductivity of the "clay exchange cations" and *w* denotes the conductivity of the "equilibrating salt solution". The coefficients *x* and *y* are "appropriate geometric constants". The bulk rock conductivity is denoted as σ_0 and is related to the petrophysical parameter bulk rock resistivity R_0 by $\sigma_0 = 1/R_0$. Similarly, $\sigma_w = 1/R_w$ where R_w is the resistivity of the formation brine. Waxman and Smits refer to the formation brine as "the free electrolyte in the pore volume of the rock" and also as an "equilibrating salt solution"[3].

Electrochemists customarily use κ to denote conductivity; Waxman and Smits use "**C"** in deference to SPE

[1] The SI and IET recommended notation for conductance is *g* or *G*, for conductivity σ, and for concentration, *c*. *Q* is the SI recommended notation for electric charge.

[2] The pedigree of this formula is traceable to Maxwell's *A Treatise on Electromagnetism*, 1873, chapter VI, paragraph 277, page 331, formula (7).

[3] "Equilibrating salt solution" is an entrenched part of the electrochemist's jargon. In formation evaluation terms it is synonymous with "formation brine". In situ, the brine would have been equilibrating with the formation for many (upwards to hundreds of millions) years. In core analysis, time up to months is allowed for equilibration.

1960s notation guidelines. We sometimes follow the Waxman and Smits notation in this appendix, but generally prefer the SI recommended notation σ for conductivity.

Note that Waxman and Smits have used the same symbol to denote both conductance and conductivity, C; this can lead to much difficulty for the reader trying to follow their derivation. However, using the SI notation, the equations are easily related. Using the relationship between conductance and conductivity, $g = (A/L)\sigma$, W-S (1) is written as

$$\frac{A_{rock}}{L_{rock}}\sigma_{rock} = \frac{A_c}{L_c}\sigma_c + \frac{A_{el}}{L_{el}}\sigma_{el}\,. \qquad \text{(A.7)}$$

When solved for σ_{rock}, this gives

$$\sigma_{rock} = \left(\frac{A_c/A_{rock}}{L_c/L_{rock}}\right)\sigma_c + \left(\frac{A_{el}/A_{rock}}{L_{el}/L_{rock}}\right)\sigma_{el}\,. \qquad \text{(A.8)}$$

Equations (A.7) and (A.8) presume, in accordance with Fig. A.1, that conductivities occupy separate (not necessarily equal) volumes. Comparing (A.8) to (A.6) the "appropriate geometric constants" x and y are

$$x = \frac{A_c/A_{rock}}{L_c/L_{rock}}\;;\quad y = \frac{A_{el}/A_{rock}}{L_{el}/L_{rock}}\,. \qquad \text{(A.9)}$$

Note that the area ratios are proportional to porosities and the length ratios are the definition of tortuosities, thus confirming their status as "geometric constants" appropriate for a parallel conductance model.

Since Eq. (A.6) gives bulk rock conductivity as a weighted average of fluid conductivities, its constants can also be evaluated petrophysically. Note that $\lim_{x\to 0}\sigma_0 = y\sigma_w$. In terms of reciprocals, this is Archie's relationship $R_0 = FR_w$. Thus $y = 1/F = \varphi_w{}^m$ where φ_w is the porosity occupied by the formation brine, which in this limit is the total porosity. Similarly, $\lim_{y\to 0}\sigma_0 = x\sigma_e$, or $x = \varphi_e{}^m$ where φ_e would be the porosity occupied by the exchange cation-filled brine, which in this limit would be, again, the total porosity. Note that the porosity exponents would in general be different for the two cases i.e., $m_w \neq m_e$. In a physical rock the latter case is not of interest (no hydrocarbon in 100% clay formation), and in the former case porosity would be shared by the formation brine in the pore bodies and "clay water" containing exchangeable cations. Thus, $\varphi_t = \varphi_e + \varphi_w$. Using this partitioning

$$\sigma_0 = \varphi_e^{m_e}\sigma_e + \left(\varphi_t - \varphi_e\right)^{m_w}\sigma_w \qquad \text{(A.10)}$$

and thus

$$x = \varphi_e^{m_e}\;;\quad y = \left(\varphi_t - \varphi_e\right)_w^{m_w}\,. \qquad \text{(A.11)}$$

So, there are at least two ways of expressing the "appropriate geometric constants" for a "parallel conductance model" as such a model is conventionally interpreted (i.e., per Maxwell's interpretation and figures A.1 and A.3). However, this is not what Waxman and Smits had in mind.

In their equation (3), Waxman and Smits write

$$x = y = \frac{1}{F^*}\quad . \qquad \text{W-S (3)} \qquad \text{(A.12)}$$

This equation introduces a problem for the parallel conductance model. If $x = y$, then according to (A.10)

$$\varphi_e^{m_e} = \left(\varphi_t - \varphi_e\right)^{m_w} \qquad \text{(A.13)}$$

This equation is satisfied when $\varphi_e = \varphi_w = \varphi_t / 2$ and $m_e = m_w \equiv m^*$. Thus with

$$x = y = \left(\frac{\varphi_t}{2}\right)^{m^*}\,, \qquad \text{(A.14)}$$

then

$$\sigma_0 = \left(\frac{\varphi_t}{2}\right)^{m^*}\left(\sigma_e + \sigma_w\right) \qquad \text{(A.15)}$$

According to the derivation above, comparing to W-S (3),

$$x = y = \left(\frac{\varphi_t}{2}\right)^{m^*} = \frac{1}{F^*}\;;\quad F^* = \left(\frac{\varphi_t}{2}\right)^{-m^*} \qquad \text{(A.16)}$$

But, according to W-S (14)

$$F^* = \varphi^{-m^*}\,. \qquad \text{W-S (14)} \qquad \text{(A.17)}$$

Eqs. (A.16) and (A.17) are in contradiction.

The coefficient of the (σ_e + σ_w) term in W-S (4) and (A.15) differ, but the terms in parentheses are the same. Thinking in terms of conventional parallel conductivity models, this is a puzzling sum. One expects to see volume-weight coefficients permitting the complementary variation of one conductivity component at the expense of the other. How can this be? Given this, and since (A.16) and (A.17) are in contradiction, something in the reasoning leading to the contradiction must be wrong.

Let's return to basics.

ELECTROCHEMISTRY

Waxman and Smits were electrochemists. If you've begun to read their paper without any preparation you know that they made no effort to connect with the practicing

formation evaluator. This job was left to Juhasz many years later (e.g., 1979, 1981). The difficulty in following the derivation of the Waxman-Smits model follows from their use of undefined terminology and unstated assumptions from electrochemistry. In addition, they seem to have misunderstood the conventional meaning, as used in electrical engineering and physics, of the term "parallel conductors". To understand their motivations and derivation a review of electrochemistry is helpful.

History. The electrochemistry of aqueous salt solutions occupied many of the 19th century's pioneering scientists[4]. In the solid state, salts are combinations of elements in columns 1 or 2 of the periodic table, the alkali metals and alkali earths, with the halogens in the 17th column. The resulting crystals are ionic, meaning that the alkali metals or alkali earths donate their outer shell electron(s) to the halogen; when the electron transfer has happened, the atoms are then called ions, with the positively charged ion known as a cation, while the negatively charged ion is called an anion.

Salts and Solutions. The simplest salts combine atoms of alkali metals with atoms of a halogen[5] in a one-to-one atomic ratio producing so-called binary salts. In the solid state these ions form a simple cubic lattice with anions and cations distributed equidistantly from each other at the corners of the lattice unit cell.

Solutions are mixtures of one or more substances dissolved in another substance. The term can be applied to solids, such as alloys, but is not usually applied to gas mixtures since gases are generally miscible, whereas solids and especially liquids, are not. Oilfield brines are aqueous solutions of salts (the solutes) in water (the solvent). Salts are ionic crystals in the solid state, but their ions can completely dissociate in water. The dissociated ions can migrate under the influence of an applied electric field, making the solutions electrically conductive.

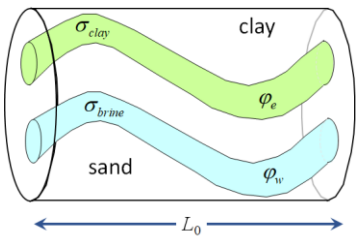

Fig. A3. A parallel conductivity model showing two separate sinuous tubes with the *same* pore geometry. The cross-sectional areas, channel lengths, pore geometries and porosities all are potentially different.

Electrical conductivity is the property of a volume that measures the ease with which mobile electrically charged particles can move under the influence of an applied electric field. Conductivity of a particular volume depends on the number of mobile charges in the volume, the amount of charge on each of the charge carriers, and the ease of particle motion in an applied electric field. Denoting conductivity of the i^{th} species of charge carriers by σ_i, considering all of these dependencies to be linear

$$\sigma_i = z_i e^{\pm} n_i \mu_i \qquad \text{(A.18)}$$

where z_i is the number of elementary charges each charge carrier bears, $e^{\pm}$ is the elementary quantum of charge (which can be negative or positive)[6], n_i is the number of charge carriers, and μ_i is the mobility of the charge carrier. In electrochemistry the quantity of charge is expressed in units of Faradays and concentrations are expressed in terms of moles per unit volume. Dividing and multiplying (A.18) by 1 in the form of N_A/N_A where N_A[7] is Avogadro's number

$$\sigma_i \propto z_i \left(N_A e^{\pm}\right)\left(\frac{n_i}{N_A}\right)\mu_i \equiv z_i \mathcal{F} Q_i \mu_i = \lambda_i Q_i . \qquad \text{(A.19)}$$

where the Faraday constant is defined by $N_A e^{+} = \mathcal{F}$ (coulomb/mol)[8] and concentration in moles per volume is $Q_i = n_i/N_A$ [mol/m^3]. The ratio of conductivity to concentration is an important parameter in electrochemistry, denoted as $\Lambda = \sigma/Q$. This ratio, called the molar conductivity, is variable, generally decreasing with increasing solute concentration. By the principle of electroneutrality, a solution contains equal amounts of opposite charge. Thus, the charge carriers in an electrolyte always comprise at least two species of ion. The molar conductivity of the solution is the sum of the molar conductivities of the individual species of ion, or $\lambda_i = z_i \mathcal{F} \mu_i$ for the i^{th} species of ion[9].

Notations. Electrochemistry employs many (confusing to the novice) notations. We have introduced the basic

[4] And, have resulted in several Nobel prizes in Chemistry over the 20th century. Arrhenius, 1903; Ostwald, 1909; Nernst, 1920; Debye, 1936; Onsager, 1968; Marcus 1992. Some of the prizes were awarded many years following the research, and some were awarded for discoveries other than in electrochemistry.

[5] "halogen" is from Greek, meaning "salt maker".

[6] 1.602×10^{-19} coulomb per electron or proton.

[7] 6.022×10^{23} ions / mole as used here.

[8] 96,485 coulomb / mole of elementary charge.

[9] Observe how easily conductivity is derivable axiomatically in terms of charge, and to consider how, or even whether, this could be done for resistivity.

quantity of solution electrochemistry as molar conductivity, denoted by Λ. Molar conductivity is defined as the ratio of conductivity to solute concentration, symbolized by

$$\Lambda \equiv \sigma / Q \text{ [10]} \qquad \text{(A.20)}$$

where concentration Q is in moles per unit volume, and σ is conductivity in siemens per unit length (the conventional notation for conductivity in electrochemistry is κ; Waxman and Smits use "$\mathfrak{C}$"; here we use the σ since this is the SI recommended and commonly used notation in physics and engineering literature). For salts in aqueous solution, the bulk conductivity depends on all ionic species dissolved in the solvent. Waxman and Smits consider only sodium chloride (z = 1), a so-called binary salt. In terms of the molar conductivities of the individual ions,

$$\Lambda_{\mathrm{NaCl}} \equiv \frac{\sigma_{\mathrm{Na}}}{Q_{\mathrm{Na}}} + \frac{\sigma_{\mathrm{Cl}}}{Q_{\mathrm{Cl}}} = \lambda_{\mathrm{Na}} + \lambda_{\mathrm{Cl}} \qquad \text{(A.21)}$$

where the λ notation for the individual ion molar conductivity ratios is conventional. For a binary salt, the concentrations of ions are identical; however, the molar conductivities and partial conductivities σ_{Na} and σ_{Cl} are controlled by the ion species' mobility and are different. These quantities are all related by the formulas

$$\lambda^{+}_{\mathrm{Na}} = \frac{\sigma_{\mathrm{Na}}}{Q_{\mathrm{Na}}} = \mathcal{F}\mu^{+}_{\mathrm{Na}} \;; \quad \lambda^{-}_{\mathrm{Cl}} = \frac{\sigma_{\mathrm{Cl}}}{Q_{\mathrm{Cl}}} = \mathcal{F}\mu^{-}_{\mathrm{Cl}} \qquad \text{(A.22)}$$

where the ion mobilities are denoted by μ and are different for different ions. Ion mobilities vary from ion-to-ion due to the different sizes, shapes, and charge numbers of the ions. The mobility is also influenced by the degree of hydration of ions; that is, how many water molecules do they tend to entrain while moving through a solution. The mobilities also depend upon the particular solvent, but water is the solvent for brines. The unit of mobility is speed per unit potential gradient. In SI units these are meter/second per volt/meter.[11]

KOHLRAUSCH LAW

Limiting molar conductivity. For salts that are completely dissociated by the action of water, individual ions may still interact electrically. For example, when an anion and cation are in close association they partially or completely neutralize each other, effectively reducing the conductivity of the solution. This "ion-pairing" is most likely to happen in concentrated solutions; it reduces the conductivity of the bulk solution. However, for dilute solutions ion-ion encounters are rare, and molar conductivity increases with decreasing concentration (or increasing dilution). The limiting value of molar conductivity at "infinite" dilution is known as the limiting molar conductivity and is characteristic of each salt solution. For example, the limiting molar conductivity for KCl in aqueous solution is ≈ 149.9 [S/m / mol/m^3][12] whereas for NaCl it is ≈ 126.45 [S/m / mol/m^3]. Since the chloride ion is the same in both solutions, the difference is attributable to the different molar conductivities (or mobilities) of potassium and sodium ions in solution.

The Kohlrausch law of independent migration of ions asserts the limiting molar conductivity of an electrolyte, is equal to the sum of the amount of each constituent ion's limiting molar conductivity. Thus

$$\Lambda_{\mathrm{NaCl}} = \lambda_{\mathrm{Na}} + \lambda_{\mathrm{Cl}} = \mathcal{F}\mu^{w}_{\mathrm{Na}} + \mathcal{F}\mu^{w}_{\mathrm{Cl}} = \frac{\sigma_w}{Q_{\mathrm{NaCl}}}, \qquad \text{(A.23)}$$

and this implies that

$$\sigma_w = \left(\lambda_{\mathrm{Na}} + \lambda_{\mathrm{Cl}}\right) Q_{\mathrm{NaCl}} = \mathcal{F}\left(\mu^{w}_{\mathrm{Na}} + \mu^{w}_{\mathrm{Cl}}\right) Q_{\mathrm{NaCl}} . \qquad \text{(A.24)}$$

This equation is not to be found in the Waxman-Smits paper, but it is implied in W-S equation (4)

$$\sigma_0 = \frac{1}{F^*}\left(\sigma_e + \sigma_w\right). \qquad \text{W-S (4)} \qquad \text{(A.25)}$$

and is illustrated in Fig. A.4. In their equation (5), W-S make explicit use of the molar conductivity of the sodium cation, writing

$$\sigma_e = \frac{\mathcal{F}\mu^{e}_{\mathrm{Na}}}{1000} Q_v = \frac{\lambda^{e}_{\mathrm{Na}}}{1000} Q_v \qquad \text{W-S (5)} \qquad \text{(A.26)}$$

where Q_v is the concentration of sodium cations associated with clay surfaces. Although it is not mentioned in their paper, the Kohlrausch Law of Independent Ion Migration is the foundation of the Waxman-Smits model; they seem to have believed that this reflected an instance of "parallel conduction". However, parallel conduction from the time of Maxwell is understood in physics and electrical engineering as something else.

W-S (4) & *W-S* (5)**.** Waxman and Smits equations (4) and (5) are worthy of some discussion. First is the factor of 1/1000. It goes uncommented upon in the W-S text, so if you don't know where it is coming from you will not be

[10] Note that a modified version of this quantity is denoted by B in the W-S model and β in the dual water model. W-S refer to this as equivalent conductance, corrected by CCD to "equivalent conductivity".

[11] In the literature these units are usually algebraically reduced to the combination [m^2 / volt/sec]. This reduction totally obscures the provenance of the unit and is not very memorable.

[12] These units are usually reduced to the less interpretable [S-m^2/mol].

enlightened by the paper[13]. In fact, it is a conversion factor for Q_v. W-S measure concentration in units of equivalents (i.e., moles of elementary quantum of charge) per liter. However, the unit used for σ_e is S/cm, the unit for μ is [cm/sec / volt/cm], and the unit for λ is [S/cm / mol/cm^3]. Therefore, the unit of concentration needed for compatibility in the formula is equivalents per cm^3. Since there are 1000 cm^3 in a liter, they divide their laboratory concentration unit by 1000 to convert the volume from liters to cm^3. This would have been much more transparent had it been rendered as

$$\sigma_e = \mathcal{F}\mu^e_{\mathrm{Na}}\frac{Q_v}{1000} = \lambda^e_{\mathrm{Na}}\frac{Q_v}{1000}\ .\ \text{W-S (5)} \qquad (A.27)$$

Finally, I will mention that W-S (5) would have been better written down as

$$\sigma_e = \mathcal{F}\mu^e_{\mathrm{Na}}Q_v = \lambda^e_{\mathrm{Na}}Q_v \qquad \text{W-S (5)} \qquad (A.28)$$

since in this form the formula is not only morphologically simpler, it is also valid for *any* system of *mutually compatible* units. In particular, either centimeter-gram-second (cgs), or (SI) meter-kilogram-second (mks) can be used without modifying the form of the equation.

Lastly, W-S (5) is a *fragment* of a conductivity equation. The entire equation would be

$$\sigma_e = \left(\lambda^e_{\mathrm{Na}} + \lambda^e_{\mathrm{clay}}\right)Q_{\mathrm{Naclay}} = \mathcal{F}\left(\mu^e_{\mathrm{Na}} + \mu^e_{\mathrm{clay}}\right)Q_{\mathrm{Naclay}} \quad (A.29)$$

This relationship includes the conductivity contribution from the clay crystal itself, considered to be a "macroion," thereby honoring the principle of electroneutrality. However, since the clay crystals are part of the rock fabric, they are immobile (i.e., $\mu^e{}_{clay} = 0$) and their contribution to brine conductivity is zero. That is, defining $Q_{\mathrm{Na}clay} = Q_v$, then

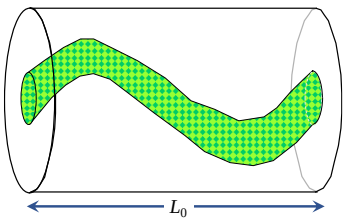

Fig. A4. In this cartoon both conductivity components are put into the same pore volume, intimately mixed. This is not the "conventional" understanding of "parallel conduction" but it does make the W-S comment regarding the "same tortuous path" decodable.

$$\sigma_e = \mathcal{F}\mu^e_{\mathrm{Na}}Q_v = \lambda^e_{\mathrm{Na}}Q_v\ .\qquad \text{W-S (5)} \qquad (A.30)$$

Returning to the discussion of Eqs. (A.30) and (A.29), for dilute solutions, the conductivities are additive. Thus, $\sigma_e + \sigma_w$ makes sense, since

$$\sigma_{brine} = \sigma_e + \sigma_w = \lambda^e_{\mathrm{Na}}Q_v + \left(\lambda^+_{\mathrm{Na}} + \lambda^-_{\mathrm{Cl}}\right)Q_{\mathrm{NaCl}}\ . \quad (A.31)$$

The concentrations can be varied independently since they are in the same container for which any geometric constants are identical. In other words, there are no volume weighting factors since both collections of ions, Q_v and Q_{NaCl}, occupy the *same volume* in the W-S model. Thus, the total conductivity σ_{brine} that results from the combination of concentrations of formation brine and clay counterions is the conductivity of a *single* conductor, not "two resistance elements in parallel". The mixture is exactly analogous to the manufacture of commercial carbon-composition resistors from a mixture of a more conductive constituent (graphite) with a less conductive constituent (dry clay) contained in a single cylindrical package.

W-S (2) appears to be a parallel conductivity model, mixing two separate components of differing conductivity with weighting coefficients, x and y, that are in general different, $x \neq y$ for a parallel conductivity model. They are related in the sense that as x increases, y correspondingly must decrease. However, although they are separate, they *can* be equal. But, although equal, they are not the same.

Thus, the W-S (3) "appropriate geometric factors" being set equal, $x = y$, which would mean two separate but identical conductors in a parallel conductor model. However, the Waxman-Smits model works only if W-S (3) implies identity; viz. $x \equiv y$. That is, y is not different from but *equal* to x, *y is x*, a *different name* for the *same volume*. Once this is appreciated, one understands why porosity closure ($\varphi_t = \varphi_e + \varphi_w$) is not invoked in the derivation of the model.

Thus is explained the statement "we assume next that the electric current transported by the counterions associated with the clay travels along the same tortuous path as the current attributed to ions in the pore water". In a parallel conduction model this statement makes no sense, especially since the point of creating such a model is to treat the two conducting volumes separately.

Waxman and Smits might alternatively have introduced their model as being analogous to Archie's model except for having a modified formation brine resistivity, since

[13] As one reads this article it becomes apparent that it was written by electrochemists for electrochemists. This explains why the authors use electrochemical jargon without explanation, and why the paper is so difficult for formation evaluators to read with understanding.

that is the final result. Indeed, this was how Juhasz explained the model to the formation evaluation community.

In conclusion a final observation can be made. The model's fundamental equation for clay counterion conductivity (W-S (5)) is valid only for dilute brines and therefore would not apply to most oil-reservoir brines. The model's region of applicability would be for very dilute formation brines where the clay counterions are most free to expand into the volume surrounding the clay crystals approaching their most dilute concentration, corresponding to the curved segment of the C_0-C_w plots featured in this article.